Results in Engineering 21 (2024) 101757

Contents lists available at ScienceDirect

Results in Engineering

journal homepage: www.sciencedirect.com/journal/results-in-engineering

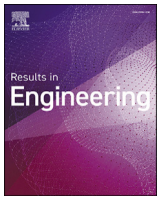

Full Length Article

Fractional-order model identification based on the process reaction curve: A unified framework for chemical processes

Juan J. Gude [a,*], Pablo García Bringas [b], Marco Herrera [c], Luis Rincón [c], Antonio Di Teodoro [c], Oscar Camacho [c]

[a] Department of Computing, Electronics and Communication Technologies, Faculty of Engineering, University of Deusto, 48007, Bilbao, Spain
[b] Department of Mechanics, Design and Industrial Management, Faculty of Engineering, University of Deusto, 48007, Bilbao, Spain
[c] Colegio de Ciencias e Ingenierías "El Politécnico", Universidad San Francisco de Quito USFQ, Quito 170157, Ecuador

ARTICLE INFO

Keywords:
Optimization
Fractional first-order plus dead-time model
Fractional-order systems
Process identification

ABSTRACT

This study introduces a novel method for identifying dynamic systems aimed at deriving reduced-fractional-order models. Applicable to processes exhibiting an S-shaped step response, the method effectively characterizes fractional behavior within the range of fractional orders ($\alpha \in [0.5, 1.0]$). The uniqueness of this approach lies in its hybrid nature, combining one-variable optimization techniques for estimating the model fractional order α with analytical expressions to estimate parameters T and L. This hybrid approach leverages information from the reaction curve obtained through an open-loop step-test experiment. The proposed method demonstrates its efficacy and simplicity through several illustrative examples, showcasing its advantages over established analytical and optimization-based techniques. Notably, the hybrid approach proves particularly advantageous compared to methods relying on the process reaction curve. To highlight its practical applicability, the identification algorithm based on this hybrid approach is implemented on hardware using a microprocessor. The experimental prototype successfully identifies the First-Order Plus Dead Time (FFOPDT) model of a thermal-based process, validating the proposed method's real-world utility.

1. Introduction

In industrial control, it is important to know the dynamic characteristics of the process to design and tune the control loop controller. These data are typically collected from a simplified mathematical model [1,2]

In this framework, the reduced-order model of the controlled process to be considered must be chosen with two important aspects in mind: (a) it must be simple to estimate, and (b) it must provide information that is reliable for predicting the effect of the control system on the controlled variable's behavior at the operating point [3].

It is widely known in the industrial and academic communities that the proportional-integral-derivative (PID) controller is still the most commonly used in industrial control applications; see [4,5]. In addition, it is common to use first-order, double-pole, and second-order plus dead-time models (FOPDT, DPPDT, and SOPDT) to tune this type of controller [6]. However, reduced-order models that precisely identify processes are sometimes required to improve control loop performance. See, e.g., [7], where it is asserted that more precise models can be used to obtain optimal PID tuning rules.

In the past few decades, fractional-order calculus and new computational approaches have made possible the gradual adoption of new identification procedures in modeling those processes that non-integer differential equations can describe [8,9]. As a result, fractional models are increasingly used in industrial applications. See [10], where a comprehensive review of fractional-order systems in automatic control is reported.

It is well-known that the FOPDT model has been extensively employed in practical applications to characterize the dynamics of real-life processes to design control systems [4]. Therefore, the fractional first-order plus dead-time (FFOPDT) model is the most natural approach to generalizing the classical FOPDT model [11].

The technical literature presents an emerging scope of methods for the identification of fractional-order models using the process reaction curve. An approach for fractional-order models with a wide range of

* Corresponding author.
E-mail addresses: jgude@deusto.es (J.J. Gude), pablo.garcia.bringas@deusto.es (P. García Bringas), marco.herrera@ieee.org (M. Herrera), lrincon@usfq.edu.ec (L. Rincón), nditeodoro@usfq.edu.ec (A. Di Teodoro), ocamacho@usfq.edu.ec (O. Camacho).

https://doi.org/10.1016/j.rineng.2024.101757
Received 19 November 2023; Received in revised form 2 January 2024; Accepted 4 January 2024
Available online 8 January 2024
2590-1230/© 2024 The Author(s). Published by Elsevier B.V. This is an open access article under the CC BY-NC-ND license (http://creativecommons.org/licenses/by-nc-nd/4.0/).

Abbreviations & Symbols

ABC	artificial bee colony
C	Caputo
CRONE	robust control of non-integer order
DPPDT	dual-pole plus dead-time
FOPDT	first-order plus dead-time
FFOPDT	fractional first-order plus dead-time
GWO	grey wolf optimizer
ML	Mittag-Leffler
MINLP	mixed integer nonlinear programming
MSE	mean squared error
GL	Grunwald-Letnikov
PI	proportional integral
PID	proportional integral derivative
PLC	programmable logic controller
PSO	particle swarm optimization
RL	Riemann-Liouville
RSM	response surface methodology
SOPDT	second-order plus dead-time
WOA	whale optimizer algorithm
α	FFOPDT model fractional order
Γ	Gamma function
θ	vector of FFOPDT model parameters
$\frac{d^n}{dt^n}$	classical n-order derivative
${}_aD_t^{\alpha}$	non-integer order derivative operator
${}_C D_{a^+}^{\alpha}$	Caputo fractional derivative
${}_{RL}D_{a^+}^{\alpha}$	Riemann-Liouville fractional derivative
Δx_{31}	distance in % between points x_3 and x_1
Δu	amplitude of the input signal
Δy	amplitude of the output signal
$e(t)$	error signal
E_{α}	one-parameter Mittag-Leffler function
$E_{\alpha,\beta}$	two-parameter Mittag-Leffler function
${}_0I_t^{\alpha}$	fractional integral of order α
J	objective function
K	process gain
L	apparent deadtime
N_S	number of samples
$N_S T_S$	time duration of the dynamic response
S	time-domain fitting criterion
t_x	time to reach x point
τ_x	normalized time to reach x point
T	time constant
T_S	sampling period
$u(t)$	control signal
$y_{\alpha}(t)$	process output signal
$\tilde{y}_{\alpha}(t)$	normalized process output signal

identification methods employs an open-loop test; for instance, the identification methods presented in [12]. These identification procedures need minimal information about the process, which makes them very common and suitable for their application in industry. One of the pioneering works in the identification of fractional-order models is the one presented by Tavakoli-Kakhki in [13], where some strategies are proposed to estimate the parameters of the FFOPDT model using step response data. These strategies combine graphical estimation and numerical computation. Estimation methods based on integration were suggested in [14] and [15] by the same author. These methods are characterized by their robustness to measurement noise.

Specifically, the most widespread approach in industrial practice relies on nonlinear optimization. These techniques seek to minimize the error between the step response of the estimated model and the process reaction curve. Reference [16] identified fractional-order models by curve fitting and analytical solutions in the time domain given by the Mittag-Leffler (ML) function. [17] identified fractional models from individual step-test data using an integral equation approach. [18] identified FFOPDT models from step response measurement using Mittag-Leffler and Grunwald-Letnikov (GL) methods. [19] identified fractional-order models using the CRONE approach, which are used to design fractional-order PI and PID controllers in [20].

More recently, renewed interest has been focused on extending integer-order model identification procedures to the fractional-order case. More specifically, several recent works extend identification methods based on the reaction curve to the case of fractional-order models. The main motivation is that they are simple and easy-to-apply procedures, and the physical interpretation of the process step response is straightforward. In this context, an identification procedure for FFOPDT models using three arbitrary points on the process reaction curve (x_1-x_2-x_3%) [21] was introduced by Gude and García Bringas. Reference [22] suggested a simplification of the previous procedure, considering the symmetry of the three points on the reaction curve of the process (x-50-(100 − x)%). Both methods are applicable to processes with overdamped response when applied to an open-loop step-input signal. The accuracy of the identified model has also been shown to be dependent to the points' positions on the process reaction curve, and [21] provides empirical rules of thumb for the selection of a set of points. Based on this idea, the effect of displacing the central point x_2 while keeping the existing symmetry between the extreme points (x_1 and x_3) has been studied in [23]. It has also been found how an identified model can be estimated more accurately. The approach proposed in [24] combines obtaining the fractional order of the model using the asymptotic property of the Mittag-Leffler function with time-based parameter estimation by considering two arbitrary points (x_1 and x_3) on the process reaction curve.

All these techniques are characterized by simplicity of application and significantly less computational effort compared to optimization-based methods. Regarding hardware implementation of identification procedures, [25] presents the conceptualization of a practical and efficient control hardware architecture intended to implement integer- and fractional-order identification and control algorithms. The effectiveness and applicability of the proposed control hardware architecture has been verified by implementing the proposed identification algorithms in [21], [22], [23], and [24] under different control technologies.

This paper introduces a novel approach to identify fractional-order models using information extracted from the reaction curve of the process. This approach is applicable to processes with overdamped step response. This method enables the estimation of the fractional order in a range $\alpha \in [0.5, 1.0]$ for processes with fractional behavior, as defined in [26]. The hybrid approach considered in this work provides the fractional order of the model by means of an optimization technique and estimates the parameters T and L by analytical techniques using two points (x_1-x_3%). The process gain K is estimated using the conventional method for integer-order models. Several illustrative examples will be used to demonstrate the effectiveness and simplicity of the proposed method in comparison to other well-known analytical and optimization-based approaches and methods based on the process reaction curve. And finally, the hybrid approach-based identification algorithm proposed in this paper will also be implemented on hardware based on microprocessor to verify its suitability and applicability for the identification of the FFOPDT model of a temperature-based process in an experimental prototype.

Motivated by the above, the contributions of this study can be summarized as follows:

1. The proposed procedure presents a novel hybrid approach that combines the estimation of α parameter by optimization-based techniques with the estimation of K, T, and L parameters by analytical techniques.
2. This hybrid approach improves the accuracy of the identified fractional-order model with a lower computational effort than other options only based on optimization techniques.
3. The algorithm developed includes the search for the optimal value of a single parameter, that is, fractional order α. This makes it simple to implement on a hardware device.
4. The effectiveness and applicability of the proposed procedure are verified by simulation and experimental results applied on a laboratory prototype, implementing the identification algorithm on microprocessor-based hardware.

The structure of this paper is as follows. Section 2 presents some preliminaries and a theoretical background. In Section 3, a novel hybrid approach of the FFOPDT model identification method is derived employing the process information collected from the reaction curve. Several experimental tests and numerical simulations are performed and the results are illustrated in Section 4 to verify the effectiveness and applicability of the proposed hybrid approach. Finally, Section 5 concludes this paper.

2. Theoretical background

2.1. Fractional calculus basics

In this section, some fundamental concepts and definitions of fractional calculus are presented. Introductory principles of fractional calculus can be explored in various books, including [27] and [28].

Fractional calculus can be understood as a generalization of the classical $n-$ order derivative $\frac{d^n}{dt^n}$ to a non-integer order derivative operator ${}_aD_t^\alpha$, where a and t denote the limits of operation, and α denotes the fractional order. There are several different definitions of the fractional operator; see [27,29]. The definitions used in this paper are briefly listed below for the reader's convenience.

Definition 1. The Riemann–Liouville (RL) fractional integral of order $\alpha > 0$ for function $f(t)$ is defined as [27,29–31]:

$$ {}_0I_t^\alpha f(t) \equiv {}_0\mathcal{D}_t^{-\alpha} f(t) = \frac{1}{\Gamma(\alpha)} \int_0^t \frac{f(\tau)}{(t-\tau)^{1-\alpha}}\, d\tau, \quad t \geq 0, \tag{1} $$

where $\alpha \in \mathbb{R}^+$ and $\Gamma(\cdot)$ is the Gamma function, [27,29]. Note that the subscripts 0 and t in definition (1) are the limits of operation.

With this definition, we can define the two most used definitions: First, the α-th order Riemann–Liouville definition of the fractional derivative for the given function $f(t)$ is expressed as:

Definition 2. Let $m = [\alpha]$ and $f \in L_1[a,b]$, $\alpha \geq 0$, the Riemann–Liouville fractional derivative ${}_{RL}D_{a^+}^\eta$ is represented by:

$$ {}_{RL}D_{a^+}^\eta f(t) = \left(\frac{d}{dx}\right)^m \left(I_{a^+}^{m-\eta}\right) f, \tag{2} $$

where $m \in \mathbb{Z}^+$, $m-1 < \alpha < m$.

Second, The α-th order Caputo (C) fractional derivatives of the given function $f(t)$ is defined as:

Definition 3. Let $\alpha \geq 0$, $m = [\alpha]$ and $f \in C^m[a,b]$. The Caputo fractional derivative ${}_cD_{a^+}^\alpha$ is given by:

$$ \left({}_cD_{a^+}^\alpha f\right)(t) := I_{a^+}^{m-\alpha} \left(\frac{d}{dx}\right)^m f, \tag{3} $$

whenever $\left(\frac{d}{dx}\right)^m$ represent the classical derivative.

Connection between both derivatives:

Lemma 1. *Let $\alpha \geq 0$ and $m = [\alpha] + 1$. Suppose that f is such that ${}_cD_{a^+}^\alpha$ and ${}_{RL}D_{a^+}^\alpha$ exists. Then*

$$ {}_cD_{a^+}^\alpha f = {}_{RL}D_{a^+}^\alpha f - \sum_{k=0}^{m-1} \frac{(x-a)^{k-\alpha}}{\Gamma(k-\alpha+1)} \left(\frac{d}{dx}\right)^k f(a), $$

Proof. See [29,31,32]. □

We can have the following result as a result of the preceding lemma:

Lemma 2. *Let $\alpha \geq 0$ and $m = [\alpha]$. Assume that f is such that both ${}_cD_{a^+}^\alpha$ and ${}_{RL}D_{a^+}^\alpha$ exist. Then ${}_cD_{a^+}^\alpha f = {}_{RL}D_{a^+}^\alpha f$ if and only if $\left(\frac{d}{dx}\right)^k f(a) = 0$ for $k = 0, \ldots, m-1$.*

Proof. Follow by direct calculation from the previous Lemma. □

To better understand these definitions, let's introduce the following examples.

Example 1. Consider $\alpha \in (0,1)$, $a^+ > 0$ and for $m \in \mathbb{N}$ (See [29,31,33]).

$$ \left[{}_{RL}D_{a^+}^\alpha (t-a)^{(m+1)\alpha-1}\right] = (t-a)^{m\alpha-1}, $$
$$ \left[{}_cD_{a^+}^\alpha (t-a)^{\beta-1}\right] = (t-a)^{\beta-1} \text{ if } \beta < \alpha+1 \text{ and } x > 0, $$
$$ \left[{}_{RL}D_{a^+}^\alpha (t-a)^{\alpha-1}\right] = 0 \text{ if } \alpha < 1 \text{ and } x > 0, $$
$$ \left[{}_cD_{a^+}^\alpha 1\right] = 0. $$

Remark 1. Note that $\lim_{\alpha \to 1^-} \left[{}_{RL}D_{a^+}^\alpha (t-a)^{\alpha-1}\right] = \frac{d}{dx} 1 = 0$ (the derivative of a constant in the Riemann-Liouville sense is not zero, but in the limit process is zero).

In this paper, considering Lemma 2, we can assume that ${}_{RL}D_{a^+}^\alpha = {}_cD_{a^+}^\alpha = D_{0^+}^\alpha = D^\alpha$ with appropriate initial conditions.

Additionally, in general, $\lim_{\alpha \to 0^+} D^\alpha f = f$.

2.2. The role of the Grünwald-Letnikov derivative and how it connects with the Riemann derivative

In fractional calculus, the Grünwald-Letnikov derivative is a commonly used approach to define fractional derivatives. It provides a discrete approximation to fractional derivatives. The fractional Grünwald-Letnikov derivative of a function $f(t)$, denoted as ${}_aD_t^\alpha f(t)$, is defined as:

$$ {}_aD_t^\alpha f(t) = \frac{1}{\Gamma(1-\alpha)} \sum_{n=0}^{\infty} (-1)^n \binom{\alpha}{n} f(t-na), \tag{4} $$

where, a is the step size, α is the order of the fractional derivative, Γ represents the gamma function and $\binom{\alpha}{n}$ is the binomial coefficient.

Example 2. Let's consider a simple example to calculate the fractional Grünwald-Letnikov derivative of a function. Suppose we have the function $f(t) = t^2$ and want to find ${}_0D_t^{0.5} f(t)$. Using the formula, we get:

$$ {}_0D_t^{0.5} f(t) = \frac{1}{\Gamma(1-0.5)} \sum_{n=0}^{\infty} (-1)^n \binom{0.5}{n} t^2 $$
$$ = \frac{2}{\sqrt{\pi}} \sum_{n=0}^{\infty} (-1)^n \frac{t^2}{(2n+1)!}. $$

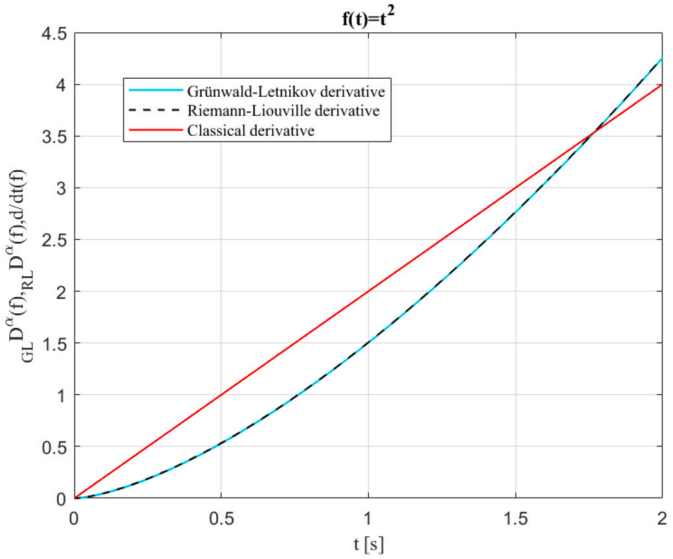

Fig. 1. Illustration of Grünwald-Letnikov, Riemann-Liouville, and classical derivatives on the function $f(t) = t^2$.

The derivative based on the definition of Grünwald-Letnikov is closely related to the Riemann-Liouville fractional derivative. The Riemann-Liouville derivative of order α is defined as:

$$ {}_0D_t^{\alpha} f(t) = \frac{1}{\Gamma(1-\alpha)} \frac{d}{dt} \int_0^t (t-\tau)^{-\alpha} f(\tau) d\tau. \tag{5} $$

The derivative based on this definition is often referred to as the discrete or discrete-time version of the Riemann-Liouville derivative in the context of fractional calculus. This means that the Grünwald-Letnikov derivative is a way to approximate and compute fractional derivatives in a discrete way.

The Grünwald-Letnikov derivative is defined as a summation over discrete data points, making it suitable for applications where data is collected at discrete time intervals. On the other hand, the Riemann-Liouville derivative is defined using an integral over a continuous interval and is more suitable for continuous-time scenarios.

The Grünwald-Letnikov derivative can be seen as a discrete approximation of the Riemann-Liouville derivative.

On the other hand, when considering the same function $f(t) = t^2$, the computation of both the Riemann-Liouville and Caputo derivatives yields ($t > 0$):

$$ {}_{RL}D_0^{\alpha} t^2 = \frac{3}{2} t^{\frac{3}{2}} $$

$$ {}_{c}D_0^{\alpha} t^2 = \frac{3}{2} t^{\frac{3}{2}} $$

Remark 2. Notice that Lemma 1 can be perfectly applied to the previous examples, highlighting the connection that exists between both derivatives and their equality for certain classes of functions

Finally, in Fig. 1, we can see how the three derivatives work.

2.3. The role of the Mittag-Leffler function and how we use

The Mittag-Leffler function plays a fundamental role in the development of fractional calculus. It can be thought of as a generalization of the exponential function and plays a crucial role in solving fractional differential equations. In this article, it is a vital component for us to find the solution to the FFOPDT model.

Definition 4. The two-parameter function of the Mittag-Leffler type, [34,35], can be defined for any given value $z \in \mathbb{C}$ as:

$$ E_{\alpha,\beta}(z) = \sum_{r=0}^{\infty} \frac{z^r}{\Gamma(\alpha r + \beta)}, \tag{6} $$

where $\beta \in \mathbb{C}$, $\alpha \in \mathbb{R}^+$, and $\Gamma(\cdot)$ denotes the Gamma function, [27,29].

Note that this function uniformly converges over the complex plane $\mathbb{C}$, exhibiting the following properties:

Let $\alpha, \beta \geq 0$

(i) If $\beta = 1$. The function aligns with the classical one-parameter Mittag-Leffler function, denoted as $E_{\alpha,1} = E_{\alpha}$. This function is defined for any arbitrary value z as follows:

$$ E_{\alpha}(z) = \sum_{r=0}^{\infty} \frac{z^r}{\Gamma(\alpha r + 1)}, \tag{7} $$

(ii) If $\alpha = 1$ and $\beta = 1$. The function is the exponential.

$$ E_{1,1}(z) = E_1(z) = exp(z) \tag{8} $$

(iii) If $\alpha = 1$ and $\beta = \frac{1}{2}$

$$ E_{\frac{1}{2},1}(z) = E_{\frac{1}{2}}(z) = exp(z^2)\,\mathrm{erfc}(-z) \tag{9} $$

Example 3. Consider $\alpha > 0$ and $\lambda \in \mathbb{C}$, then ${}_{RL}D_0^{\alpha} E_{\alpha}(\lambda t^{\alpha}) = \lambda E_{\alpha}(\lambda x^{\alpha})$. See [31,36]

Remark 3. In this paper, for the sake of simplicity, we assume the same variable t for both functions and their derivatives, lightly abusing the notation. "We do not use: $({}_{RL}D_0^{\alpha} f(t))(x) = g(x)$"

2.4. Overview of the fractional-order model identification method based on fitting three arbitrary points on the process reaction curve

In this section, an overview of the identification procedure to be used as the basis for the hybrid approach proposed in this paper is presented.

The transfer function for a typical FFOPDT model is as follows:

$$ P(s) = \frac{Y_{\alpha}(s)}{U(s)} = \frac{K e^{-Ls}}{1 + T s^{\alpha}} \tag{10} $$

where $u(t)$ is the input signal, which is usually the control signal, and $y_{\alpha}(t)$ is the output signal, which is usually the variable to be controlled.

FFOPDT model parameters are $\theta = \{K, T, L, \alpha\}$, where K is the process gain, $T > 0$ the time constant, $L \geq 0$ the apparent deadtime, and α the non-integer order of the model. This model can be considered as the natural generalization to non-integer orders of the classical FOPDT model [11], widely utilized in practical applications to approximate the dynamics of numerous industrial processes for control purposes [4].

The general FFOPDT model identification procedure for characterizing processes with S-shaped response based on the process reaction curve that has been recently proposed in [21] is summarized below.

Fig. 2 illustrates the step-input signal $u(t)$ with amplitude Δu and the corresponding output signal of an FFOPDT model $y_{\alpha}(t)$, which has an amplitude variation of Δy.

FFOPDT model (10) response to a Δu step input change is:

$$ y_{\alpha}(t) = \begin{cases} 0, & 0 \leq t < L \\ K \left\{ 1 - E_{\alpha,1} \left[-\frac{1}{T}(t-L)^{\alpha} \right] \right\} \Delta u, & t \geq L \end{cases} \tag{11} $$

where the output signal change is $\Delta y = K \cdot \Delta u$.

Normalizing the process output $y_{\alpha}(t)$ with respect to the process output total change $\Delta y = K \cdot \Delta u$ and substituting the time variable t for the

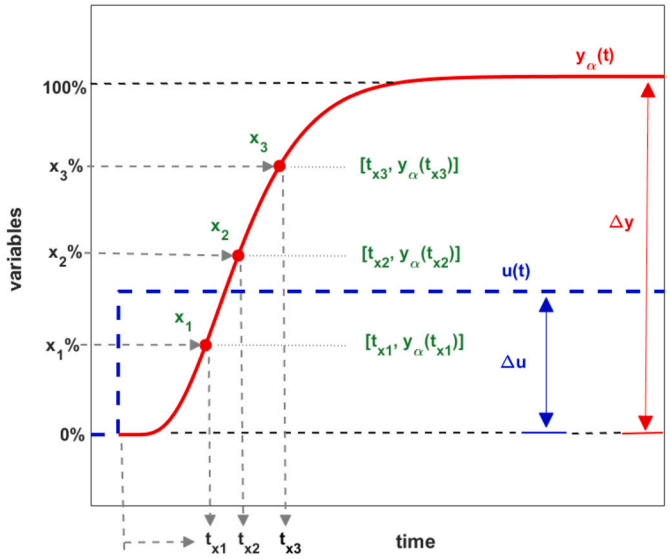

Fig. 2. Process reaction curve $y_\alpha(t)$ obtained as a response of the FFOPDT model to a step-input signal $u(t)$. Three arbitrary points $\{x_1, x_2, x_3\}$ on the process reaction curve are also shown. The parameters required to identify the fractional-order model are $\{\Delta y, \Delta u, t_{x1}, t_{x2}, t_{x3}\}$.

shifted and normalized time $\tau = \frac{1}{T}(t-L)^\alpha$, eq. (11) is reduced to the following expression:

$$\tilde{y}_\alpha(\tau) = \frac{y_\alpha(\tau)}{\Delta y} = 1 - E_\alpha(-\tau), \qquad \tau \geq 0 \tag{12}$$

where $0 \leq \tilde{y}_\alpha(\tau) \leq 1$ and depends on α and τ.

Note that the parameter τ_x is defined as the normalized time, representing the time it takes $\tilde{y}_\alpha(\tau)$ to achieve $x\%$ of the total change, corresponding to the position $(\tau_x, \tilde{y}_\alpha(\tau_x))$ on the normalized process output curve. Consequently, t_x signifies the time needed for $y_\alpha(t)$ to achieve $x\%$ of the total change, corresponding to the position $(t_x, y_\alpha(t_x))$. The relationship between t_x and τ_x is expressed as follows:

$$t_x = L + (\tau_x T)^{1/\alpha}, \tag{13}$$

According to [21], the following set of equations is obtained to estimate the FFOPDT model parameters θ using data information $\{\Delta y, \Delta u, t_{x1}, t_{x2}, t_{x3}\}$ from the process reaction curve:

$$\begin{cases} K = \frac{\Delta y}{\Delta u} \\ \alpha = f_1(\Delta) \\ T = f_2(\alpha)(t_{x3} - t_{x1})^\alpha \\ L = max[t_{x3} - f_3(\alpha)T^{1/\alpha}, 0] \end{cases} \tag{14}$$

where $\{t_{x1}, t_{x2}, t_{x3}\}$ are the set of times required to reach $x_1\%$ $(y_\alpha(t_{x1}))$, $x_2\%$ $(y_\alpha(t_{x2}))$, and $x_3\%$ $(y_\alpha(t_{x3}))$ of the process output total change, respectively, as illustrated in Fig. 2. Also note that expressions for functions $f_1(\Delta)$, $f_2(\alpha)$, and $f_3(\alpha)$ are experimentally determined by using normalized times $\{\tau_{x1}, \tau_{x2}, \tau_{x3}\}$ for $0.50 \leq \alpha \leq 1.00$. Therefore, the function f_1 relies on the ratio index Δ, determined by the normalized times τ_{x1}, τ_{x2}, and τ_{x3}; and functions f_2 and f_3 depend on α and the times τ_{x1} and τ_{x3}, and τ_{x3}, respectively.

Fig. 3 shows the overall schematic of the method for identifying the parameters of an FFOPDT model by fitting three arbitrary points (x_1-x_2-x_3%). Note that this scheme is divided into two distinct parts: Part A (in blue) consists of the general procedure for determining the rational expressions for functions $f_1(\Delta)$, $f_2(\alpha)$, and $f_3(\alpha)$, which depend on the location of the set of points (x_1-x_2-x_3%) and are obtained from the normalized times $\{\tau_{x1}, \tau_{x2}, \tau_{x3}\}$ for $0.50 \leq \alpha \leq 1.00$ using curve fitting. Thus, the set of equations (14) is obtained. Part B (in red) illustrates the identification algorithm using data extracted from the reaction curve of the process.

We refer the interested reader to [21] for a more detailed description of this identification method. Note that this procedure is based on fitting three arbitrary points (x_1-x_2-x_3%) on the reaction curve of the process, where the process information is obtained from a simple open-loop test. This reference also includes an analysis of how the location of arbitrary points (x_1-x_2-x_3%) affects the identified model's accuracy, along with providing some practical guidelines for the choice of symmetrical and asymmetrical set of representative points. In this context, [22] proposes a simplification of the previous procedure by particularizing in situations where only symmetrically positioned points on the reaction curve of the process (x-50-($100-x$)%) are selected. As stated in [23], the identified fractional-order model's accuracy is influenced by the location of the central point x_2. New insights are offered on this central point selection x_2 in the context of symmetrical identification procedure.

2.5. Brief overview of process identification optimization approaches

Optimization methods are frequently used in process model identification to estimate model parameters to identify the best-fit model for the experimental data. The following brief describes some commonly used optimization techniques in the context of process model identification.

1. Blackbox optimization: Derivative-free optimization (also known as blackbox optimization) is a mathematical optimization discipline that does not employ derivative information to discover optimal solutions [37,38].
2. Gradient Descent: Gradient descent (also known as steepest descent) is an iterative optimization method for locating the local minimum of a differentiable function by taking repeated steps in the opposite direction of the gradient. The stochastic gradient descent method is the stochastic approximation of the steepest descent method because it replaces the actual gradient (derived from the whole data set) with an estimate of the gradient (calculated from a randomly selected portion of the data). These approaches are widely utilized in science and engineering, particularly in machine learning and neural network training [39].
3. Nonlinear regression: Nonlinear regression estimates the model parameters by minimizing the difference between experimental data and the model predictions by successive approximations. The method is based on a linear approximation of the model and successive iterations to adjust the parameters. Among the various approaches, the Gauss-Newton and Levenberg-Marquardt algorithms are commonly used [40,41].
4. Mixed integer nonlinear programming (MINLP): MINLP methods are used when the optimization problem involves discrete and continuous variables, common in chemical process optimization [42].
5. Metaheuristic optimization models are global optimization approaches that can provide a good solution to an optimization problem when the information is insufficient. Natural systems have inspired several current metaheuristics, particularly evolutionary computation-based techniques. Nature provides concepts, techniques, and principles for the design of artificial computing systems to address complicated computational challenges. Such metaheuristics include simulated annealing [43,44], evolutionary algorithms [45], genetic algorithms [46], bio-inspired [47] and particle swarm optimization [48].
6. Bayesian Optimization: Bayesian optimization is a fast way to optimize expensive black-box functions that don't have any functional forms. It can be used to improve process conditions or model hyperparameters [49].
7. Response Surface Methodology (RSM): RSM models and optimizes complex processes by fitting response surfaces. It is particularly

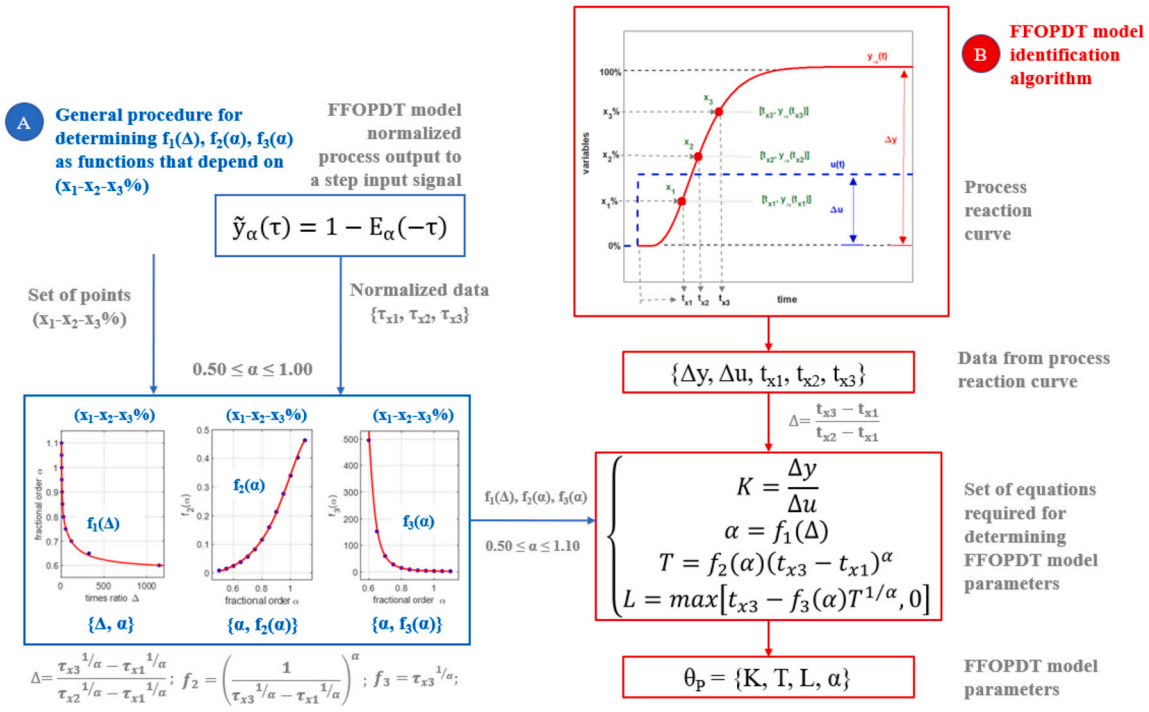

Fig. 3. Overview of the entire method for identifying an FFOPDT model considering three arbitrary points (x_1-x_2-x_3%) on the process reaction curve.

useful when experimental data are costly or time-consuming to obtain [50].

8. Neural networks: Machine learning techniques, such as neural networks, can be used for process identification and optimization when dealing with complex, high-dimensional data [51].

The optimization approach used is determined by the process's specific characteristics, the type of the data, and the available computer resources. Some problems may necessitate a combination of these strategies, and it is critical to validate the outcomes of optimization using proper statistical techniques. In the following sections, an analytical technique and a derivative-free optimization algorithm are combined to improve the parameter determination.

3. Hybrid identification approach based on the process reaction curve

As mentioned in the previous section, FFOPDT model parameters can be calculated by specifying three arbitrary points (x_1-x_2-x_3%) on the reaction curve of the process. Note that the location of these three representative points is a strict limitation on the model response constraining the whole curve.

Given that fractional order α significantly influences the behavior of the model [13], it is critical to properly estimate the value of α. It is important to mention that a good estimate of α can ensure the best fit between the step response of the FFOPDT model and the reaction curve of the process.

This section proposes a modification to the identification method summarized in the previous section that involves searching for the optimal value of α using an optimization method. The considered approach is hybrid since it combines analytical and optimization-based techniques. On the one hand, parameters K, T, and L are determined using the analytical expressions proposed in [21]. More precisely, the values of the parameters T and L are determined based on two points on the reaction curve of the process. The expressions for these parameters depend on the position of these points (x_1 and x_3) and the parameter α value. On the other hand, the estimation of the fractional order is based on the search for the optimal value of α.

In the following, we detail how to estimate the parameters of the FFOPDT model ($\theta = \{K, T, L, \alpha\}$) by using the hybrid approach proposed in this paper. This identification procedure is described as an algorithm.

3.1. Estimation of K

The method of estimating process gain K remains identical to that for conventional integer-order models, as detailed in [4]. The process gain can be estimated from data collected based on the following expression:

$$K = \frac{\Delta y}{\Delta u}, \tag{15}$$

where Δu is the step input change and Δy is the process output total change, as shown in Fig. 4.

3.2. Estimation of T and L

The normalized process output $\tilde{y}_\alpha(\tau)$ is used to determine normalized data $\{\alpha, f_2(\alpha)\}$ and $\{\alpha, f_3(\alpha)\}$ for $\alpha \in [0.5, 1.0]$ and fit the characteristic functions $f_2(\alpha)$ and $f_3(\alpha)$ required to estimate T and L. Fig. 4 shows the reaction curve of the process and the characteristic points x_1 and x_3 located on that curve at a distance Δx_{31} from each other. The times t_{x1} and t_{x3} needed for the estimation of T and L are also displayed.

According to [21], the analytical expressions for estimating parameters T and L in terms of t_{x1} and t_{x3}, which are the times needed for the response to achieve the representative points x_1 and x_3, are given below:

$$\begin{cases} T = f_2(\alpha)(t_{x3} - t_{x1})^\alpha \\ L = max[t_{x3} - f_3(\alpha)T^{1/\alpha}, 0] \end{cases} \tag{16}$$

Remark 1. Functions f_2 and f_3 depend on α and the normalized times τ_{x1} and τ_{x3}, and τ_{x3}, respectively, for $0.5 \le \alpha \le 1.0$. The selection of x_1 and x_3 has a significant influence on the accuracy of the model parameters. The results obtained in [22] verify that the accuracy of the FFOPDT

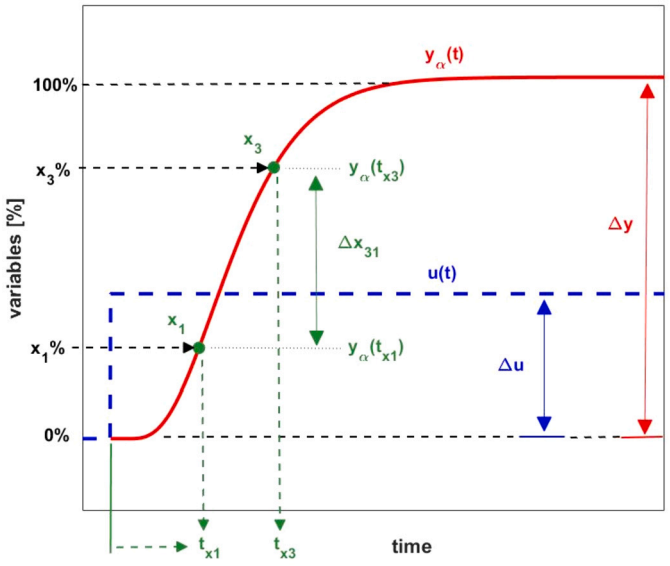

Fig. 4. Step-input signal $u(t)$, S-shaped step response signal $y_\alpha(t)$, and selected representative points x_1 and x_3 on the reaction curve of the process. The figure also illustrates process data $\{\Delta u, \Delta y, t_{x1}, t_{x2}\}$ collected from the process reaction curve, required for the identification of the FFOPDT model. $\Delta x_{31} = x_3 - x_1$ represents the distance in % between points x_3 and x_1.

model parameters is sensitive to the selection of the set of points on the process reaction curve. It is also suggested that the distance between points x_3 and x_1 (Δx_{31}) to be long to improve the accuracy of T and L. In this respect, both references [21] and [23] have provided new insights and rules of thumb for the selection of the set of points in the context of the identification procedure based on the process reaction curve.

3.3. Estimation of α

The main feature of the proposed approach consists in the estimation of α parameter, which can be formulated as a minimization problem of the following objective function:

$$J(\theta) = \min_{\alpha} \left\{ \sum_{k=1}^{N_S} \left[e(kT_S, \theta) \right]^2 \right\} = \min_{\alpha} \left\{ \sum_{k=1}^{N_S} \left[y(kT_S) - y_\alpha(kT_S, \theta) \right]^2 \right\} \tag{17}$$

where θ is the vector of FFOPDT model parameters, $e(kT_S, \theta)$ is the error, which is the difference between the process reaction curve $y(kT_S)$ and the step response of the identified model $y_\alpha(kT_S, \theta)$, N_S is the number of collected samples, and T_S is the sampling period. Note that the selected objective function is the squared error.

The above minimization problem is subject to the constraints previously considered in eq. (16).

Remark 2. As discussed above, the estimation of α parameter is based on the search for the optimal value that minimizes the cost function $J(\theta)$. The values of T and L, which are dependent on the position of the representative points x_1 and x_3, are set as constraints.

For the minimization of eq. (17) the *fminbnd* optimizer as implemented in Matlab is employed. This optimizer is based on golden section search and parabolic interpolation. The golden-section search is a method for locating the minimum of a function inside a certain interval. If the minimum is on its boundaries, the optimizer will converge to that point. The approach works by gradually decreasing the range of values on the set interval, making it extremely robust.

An interpretation of the problem could be summarized as the search for the optimal value of α that best fits the step response of the FFOPDT model to the process reaction curve, requiring the response to pass through points x_1 and x_3. The proposed hybrid approach can be seen as seeking a compromise between simplicity and accuracy of the method, requiring low computational effort compared to other methods based only on optimization. The optimal setting of α also improves the accuracy of T and L. Since f_2 and f_3 depend on α, a more precise estimation of α will result in an even more precise estimation of T and L. Note that the values of f_2 and f_3 are updated at each iteration of the algorithm, and, therefore, so are T and L.

3.4. Identification algorithm proposal

The approach proposed in this paper can be formulated as an algorithm summarized in Fig. 5 and discussed below. The procedure for obtaining the reduced-order fractional model parameters $\{K, T, L, \alpha\}$ that minimize the objective function involves initialization, main algorithm, and termination phases.

A. Initialization

This phase involves the selection of the values of x_1 and x_3 (step 1). Some insights into the selection of the representative points on the process reaction curve are provided in [21] and [22] to improve the identified fractional-order model's accuracy. Expressions for functions $f_2(\alpha)$ and $f_3(\alpha)$ considering $0.5 \leq \alpha \leq 1.0$ are also determined by curve fitting (step 2). The detail of obtaining rational functions for $f_2(\alpha)$ and $f_3(\alpha)$ from the normalized data $\{\tau_{x1}, \tau_{x3}\}$ is also illustrated in the figure. See also [24].

B. Main algorithm

This phase presents the main algorithm of an optimal approach based on the process reaction curve. It includes the following steps:

- Collect the process reaction curve vector $y(kT_S)$ with a time length $N_S T_S$ (step 3).
- Determination of times t_{x1} and t_{x3} to reach $y(t_{x1})/\Delta y = x_1/100$ and $y(t_{x3})/\Delta y = x_3/100$ (step 4).
- Initialization of the parameter $\alpha = \alpha_0 \in [0.5, 1.0]$ (step 5).
- Estimation of process gain K by using analytical expression (15) (step 6).
- Update of f_2 and f_3, as functions of α, and estimation of T and L using analytical expressions (16) (step 7).
- Estimation of α by minimization of eq. (17) using the *fminbnd* optimizer (step 8).
- Evaluate whether the objective function $J(\theta_0)$ takes its minimum value (step 9).
- In case $J(\theta_0)$ is not minimal, update $\alpha = \alpha_0^{upd}$ (step 10).

Steps 6-10 of this procedure combine the search for the optimal value of α_0 that minimizes the objective function $J(\theta_0)$, which is based on optimization, with the determination of parameters T and L using analytical expressions (16). Note that this procedure is hybrid because it combines analytical techniques (steps 6 and 7) with those based on optimization (steps 8-10). Determination of parameters T and L depends on α and, therefore, the optimal setting of α contributes to both T and L being set more accurately.

C. Termination

Depending on the user-defined step size, the nested loop runs for the required number of iterations until optimal value of α_0 is obtained. The updating set $\theta_0^{upd} = \left\{ K, T_0^{upd}, L_0^{upd}, \alpha_0^{upd} \right\}$ changes to the optimal set $\theta_0^{opt} = \left\{ K, T_0^{opt}, L_0^{opt}, \alpha_0^{opt} \right\}$ (step 11). Note that the superscript *upd* means updated and *opt* means optimal.

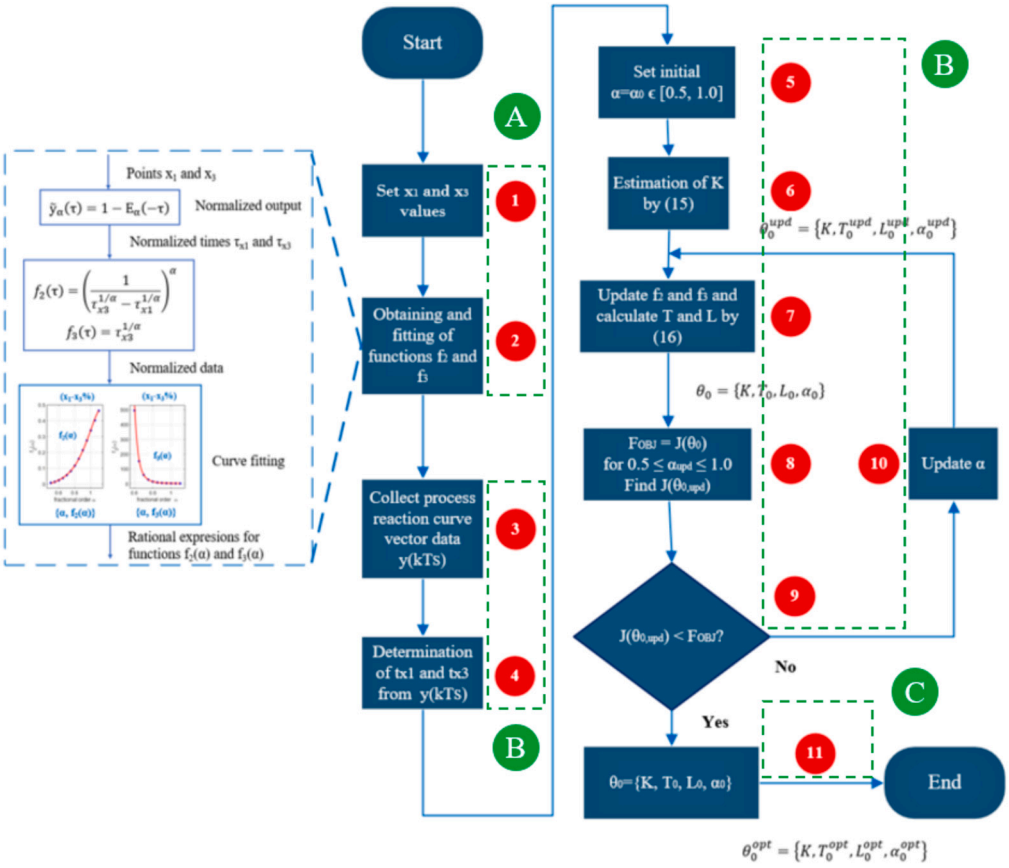

Fig. 5. Optimal approach-based FFOPDT model identification algorithm flowchart.

3.5. Some final remarks and limitations of the work

This section presents some observations and limitations of the hybrid approach proposed in this work, particularly regarding industrial practice.

The hybrid approach proposed in this paper is applied to the identification of processes exhibiting fractional behavior characterized by a monotonic S-shaped response. These processes, which are prevalent in process control [4], can be represented by an FFOPDT model with fractional order in the range $0.50 \leq \alpha \leq 1.00$.

The proposed method takes the process information from the reaction curve, which is essentially the open-loop step response. It is a fundamental tool in process control that provides information about the dynamic behavior of a system. It allows engineers to design effective control strategies, optimize performance, and ensure the stability and reliability of industrial processes [2].

In an industrial environment, it is common for the feedback signal of the controlled process to contain measurement noise. This requires appropriate filtering when the signal is used for model identification and control purposes. Given that the filter dynamics will be an integral component of the controlled process to be identified, the proposed identification procedure does not account for the noise from the measurement [52,53].

Since the dynamic characteristics of the process change with the operating point of the control loop and this can vary due to the effect of disturbances or due to a change in the setpoint, there is an implicit uncertainty in the nominal model. The main purpose of the identified fractional-order model is to design the control system, as considered above. Therefore, the usual approach is to consider the uncertainty of the model when designing the control system; see, e.g., [16,54,55]. Thus, this ensures a certain degree of robustness of the designed control system to model uncertainties.

4. Experimental results

The previous section discusses the proposed hybrid approach to identify a reduced-order fractional model based on the reaction curve. The parameters of the model are estimated by combining optimization-based methods with analytical expressions using information taken from the reaction curve of the process.

This section provides the experimental models estimated by applying the FFOPDT model identification method suggested in this work. These models have been compared with those obtained using different analytical and optimization-based identification methods proposed in the technical literature.

Although the proposed procedure is general and valid for any set of points (x_1-x_3%), the following considerations have been addressed in the experiments conducted in this section. Points x_1 and x_3 are $x_1 = x = 10\%$ and $x_3 = (100 - x) = 90\%$ without loss of generality, showing symmetry to the center of the total range and a distance between points of $\Delta x_{31} = 80\%$.

Figs. 6 and 7 show data sets $\{\alpha, f_2(\alpha)\}$ and $\{\alpha, f_3(\alpha)\}$ for $0.50 \leq \alpha \leq 1.00$, and curve fitting results for points $x_1 = 10\%$ and $x_3 = 90\%$. The fitting curves have been obtained by applying the Levenberg-Marquardt least-squares algorithm for data fitting using the following rational functions:

$$f_2 = \frac{p_1\alpha + p_2}{\alpha^2 + q_1\alpha + q2}, \tag{18}$$

$$f_2 = \frac{p_1\alpha^2 + p_2\alpha + p_3}{\alpha^2 + q_1\alpha + q2}, \tag{19}$$

The parameter values $\{p_i, q_i\}$ corresponding to the functions $f_2(\alpha)$ and $f_3(\alpha)$ in eqs. (18) and (19) are shown in Tables 1 and 2, respectively.

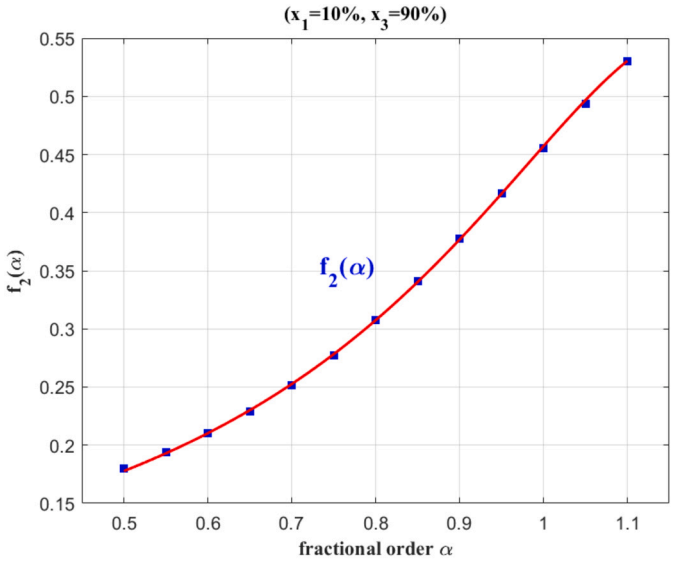

Fig. 6. Data set $\{\alpha, f_2(\alpha)\}$ for $0.5 \leq \alpha \leq 1.0$ and the result of curve fitting for $f_2(\alpha)$ considering $x_1 = 10\%$ and $x_3 = 90\%$.

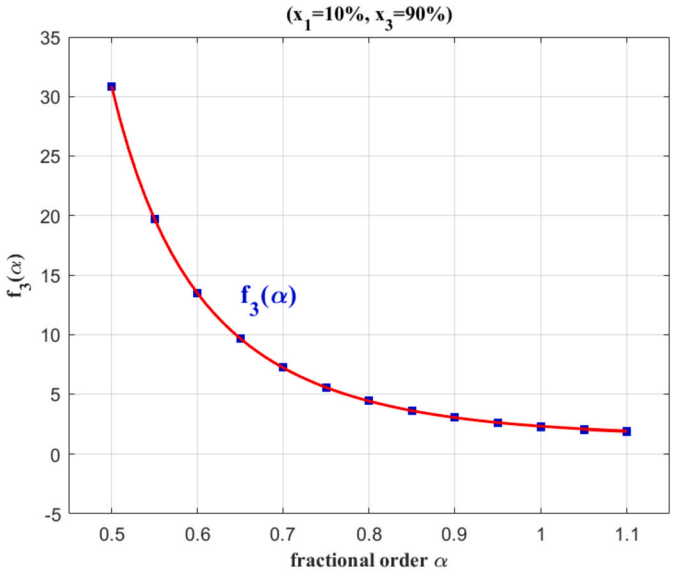

Fig. 7. Data set $\{\alpha, f_3(\alpha)\}$ for $0.5 \leq \alpha \leq 1.0$ and the result of curve fitting for $f_3(\alpha)$ considering $x_1 = 10\%$ and $x_3 = 90\%$.

Table 1
Parameters $\{p_i, q_i\}$ of the rational function $f_2(\alpha)$ for set of points $x_1 = 10\%$ and $x_3 = 90\%$.

$(x_1\text{-}x_3)$	p_1	p_2	q_1	q_2
$x_1 = 10\%, x_3 = 90\%$	−0.0673	0.1578	−2.501	1.699

Table 2
Parameters $\{p_i, q_i\}$ of the rational function $f_3(\alpha)$ for set of points $x_1 = 10\%$ and $x_3 = 90\%$.

$(x_1\text{-}x_3)$	p_1	p_2	p_3	q_1	q_2
$x_1 = 10\%, x_3 = 90\%$	4.066	−7.705	5.055	−0.4136	0.02868

The set of equations (16) can be modified for this particular set of points $(x_1\text{-}x_3)$ as follows:

$$\begin{cases} T = f_2(\alpha)(t_{90} - t_{10})^{\alpha} \\ L = max[t_{90} - f_3(\alpha)T^{1/\alpha}, 0] \end{cases} \tag{20}$$

where $x_1 = 10\%$ and $x_3 = 90\%$, and data information taken from the reaction curve required to identify the FFOPDT model is $\{\Delta y, \Delta u, t_{10}, t_{90}\}$.

The time-domain fitting criterion that has been used to evaluate the accuracy of the identified models is the mean squared error (MSE):

$$S(\theta) = \frac{1}{N_S}\sum_{k=1}^{N_S}[e(kT_S, \theta)]^2 = \frac{1}{N_S}\sum_{k=1}^{N_S}[y(kT_S) - y_m(kT_S, \theta)]^2, \tag{21}$$

where θ is the vector of process model parameters, N_S is the number of samples collected, T_S is the sampling period, $N_S T_S$ is the time duration of the dynamic response, and $e(kT_S, \theta)$ is the difference between the process reaction curve and the step response of the identified model, denoted as $y(kT_S)$ and $y_m(kT_S, \theta)$, respectively.

The examples in this section are used to determine the superiority of the proposed method compared to analytical methods. Moreover, one of the outstanding features of the hybrid identification method is that it finds a compromise between the accuracy of the identified model and the computational effort in its implementation. The first two examples are also used to compare the proposed hybrid approach with other optimization-based methods. The last example is used to demonstrate the applicability of the proposed identification procedure and its implementation on microprocessor-based hardware when applied to a laboratory prototype.

The first two examples were conducted using Matlab 2019b software on a Windows 10 PC equipped with an Intel®, Core™ $i7-7500U$ processor running at 2.9 GHz. FOTF toolbox [56], which provides many built-in Matlab functions to handle fractional systems, was used to simulate fractional order models. When configuring the optimization algorithms, we used an initial population of 50 search agents and set a maximum limit of 70 iterations. Example 3 was developed using the hardware architecture described in [25]. This was carried out using LabVIEW and implemented on the NI myRIO platform microprocessor, which boasts a 667 MHz dual-core ARM®, Cortex™-A9 processor. The sampling period is $T_S = 0.1$ s, and the number of samples N_S for the examples is indicated in each experiment.

This section is divided as follows. Sections 4.1 and 4.2 present the results obtained using two fractional-order process models. Section 4.3 shows the results obtained by applying the proposed hybrid approach to a thermal process-based hardware-in-the-loop experimental setup. Finally, Section 4.4 discusses the experimental results obtained in the previous sections.

4.1. Example 1

This example selects a fractional-order process model dominated by higher-order lag [13]:

$$P_1(s) = \frac{K_1}{\prod_{i=1}^{3}(1 + T_i s^{\lambda_1})}, \tag{22}$$

where $K_1 = 3$, $T_1 = 3$ s, $T_2 = 2$ s, $T_3 = 1$ s, and $\lambda_1 = 0.88$.

In this case, the FFOPDT model estimated considering the suggested identification method is contrasted with models estimated with other identification procedures.

Firstly, the FFOPDT model is estimated using the suggested identification procedure. An open-loop step-test experiment is applied to the process P_1 to obtain the process reaction curve, as illustrated in Fig. 8. Table 3 presents process data needed to apply the proposed identification approach with the selected set of points (10-90%).

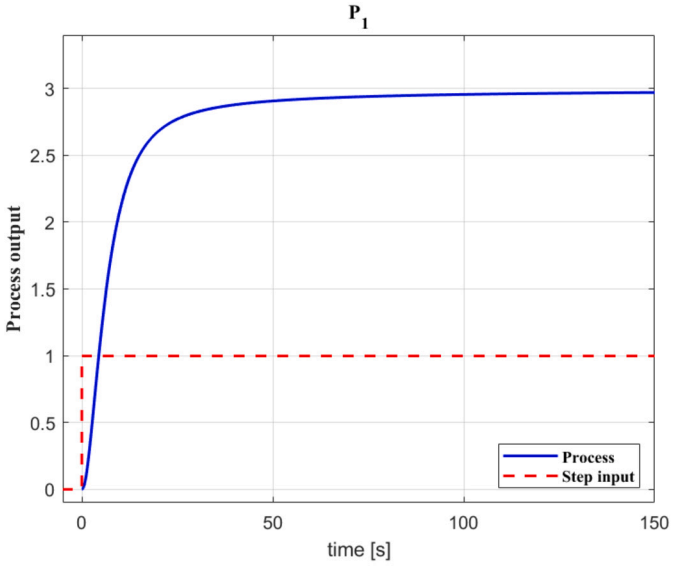

Fig. 8. Result of the open-loop step-test experiment applied to process P_1: Step-input signal and process reaction curve.

Table 3
Process information obtained from the process reaction curve and required for FFOPDT model identification of process P_1.

Process $P_1(s)$
Proposed method ($x_1 = 10\%$, $x_3 = 90\%$)
$\Delta u = 1.00$
$\Delta y = 3.00$
$t_{10} = 2.0290$ s
$t_{90} = 20.8030$ s

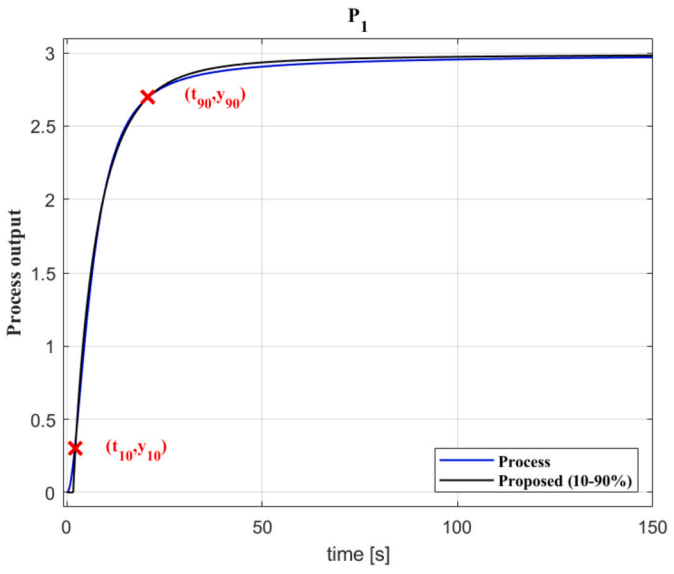

Fig. 9. Step response of the FFOPDT model estimated with the suggested identification procedure and reaction curve of the process P_1. Points $x_1 = 10\%$ and $x_3 = 90\%$ are also included in the figure for illustrative purposes.

Fig. 9 shows the comparison between the reaction curve of the process P_1 and the corresponding step response of the FFOPDT model estimated using the suggested identification method.

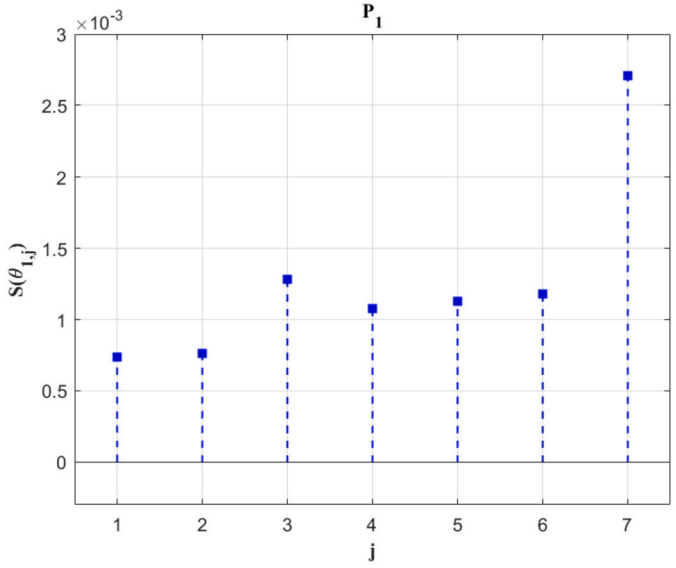

Fig. 10. Illustration of the performance index values $S(\theta_{1,j})$ determined with the models estimated using different identification methods for process P_1.

In addition, several FFOPDT and FOPDT models have also been obtained considering various integer- and fractional-order model identification methods. More precisely, FFOPDT models have been obtained using the process reaction curve-based methods proposed by Gude et al. in [24], and in [21] for the symmetrical set (10-50-90%) and for the asymmetrical set (10-55-90%), respectively. FFOPDT models using the procedure described by Tavakoli-Kakhki in [13] and the one estimated using the optimization-based method followed by Guevara et al. in [19] have also been obtained. Finally, the optimal parameters for the FOPDT model have also been estimated.

Table 4 shows model parameters $\theta_{1,j} = \{K_{1,j}, T_{1,j}, L_{1,j}, \alpha_{1,j}\}$ for $j = 1, ..., 7$, which have been obtained using the corresponding identification methods mentioned above.

The values of $S(\theta_{1,j})$ have been calculated for the models estimated using the different identification procedures ($j = 1, ..., 7$) applied to the process P_1. These values provide an evaluation of the identified models' accuracy, as illustrated in Fig. 10 and in Table 5. Additionally, Table 6 and Fig. 11 show the relative performance index values $S_{1,j} = S(\theta_{1,1})/S(\theta_{1,j})$ for the different models ($j = 1, ..., 7$) compared to that obtained with the proposed method ($j = 1$). This figure illustrates that the proposed method reduces the value of S by 3%, 42%, 31%, 34%, 37%, and 73% compared to the procedures proposed by Gude with the Mittag-Leffler based method, for the symmetrical method, for the asymmetrical method, the method by Tavakoli-Kakhki, the one by Guevara, and for the optimal FOPDT model, respectively.

In addition, the FFOPDT model parameters have also been estimated using several optimization-based identification methods. More specifically, the following optimization techniques have been used to determine FFOPDT model parameters: Artificial Bee Colony (ABC), Grey Wolf Optimizer (GWO), Particle Swarm Optimization (PSO), and Whale Optimizer Algorithm (WOA).

Table 7 contains the parameters of the FFOPDT model $\theta_{1,j} = \{K_{1,j}, T_{1,j}, L_{1,j}, \alpha_{1,j}\}$ for $j = 1, ..., 5$, which have been estimated using the different optimization-based techniques mentioned above.

In Table 8, the values of the model performance index in the time domain $S(\theta_{1,j})$ have been calculated for the models estimated using the different identification methods ($j = 1, ..., 5$) applied to the process P_1. Information on the execution time of optimization-based procedures has also been included to give insight into the computational effort of each method. This table illustrates that the proposed method provides a more accurate model than the one obtained using the WOA technique, while the models obtained with the remaining techniques are more accurate

Table 4
FFOPDT model parameters for the process P_1 estimated using various identification techniques ($j = 1, ..., 6$) and parameters estimated for an optimal FOPDT model ($j = 7$).

j	Technique	FFOPDT model parameters $\theta_{1,j}$			
1	Proposed	$K_{1,1} = 3.00$	$T_{1,1} = 5.69$ s	$L_{1,1} = 1.50$ s	$\alpha_{1,1} = 0.915$
2	Gude Mittag-Leffler [24]	$K_{1,2} = 3.00$	$T_{1,2} = 5.81$ s	$L_{1,2} = 1.51$ s	$\alpha_{1,2} = 0.920$
3	Gude Symmetrical [21]	$K_{1,3} = 3.00$	$T_{1,3} = 6.64$ s	$L_{1,3} = 1.39$ s	$\alpha_{1,3} = 0.947$
4	Gude Asymmetrical [21]	$K_{1,4} = 3.00$	$T_{1,4} = 6.38$ s	$L_{1,4} = 1.43$ s	$\alpha_{1,4} = 0.939$
5	Tavakoli-Kakhki [13]	$K_{1,5} = 3.00$	$T_{1,5} = 6.30$ s	$L_{1,5} = 1.00$ s	$\alpha_{1,5} = 0.920$
6	Guevara [19]	$K_{1,6} = 3.00$	$T_{1,6} = 5.63$ s	$L_{1,6} = 1.88$ s	$\alpha_{1,6} = 0.926$
7	Optimal FOPDT	$K_{1,7} = 3.00$	$T_{1,7} = 8.74$ s	$L_{1,7} = 0.00$ s	–

Table 5
Time-domain performance index values $S(\theta_{1,j})$ determined using the models estimated using different identification procedures for the process P_1.

j	Technique	Set of points	$S(\theta_{1,j})$
1	Proposed	(10-90%)	$7.39 \cdot 10^{-4}$
2	Gude Mittag-Leffler	(10-90%)	$7.63 \cdot 10^{-4}$
3	Gude Symmetrical	(10-50-90%)	$1.28 \cdot 10^{-3}$
4	Gude Asymmetrical	(10-55-90%)	$1.08 \cdot 10^{-3}$
5	Tavakoli-Kakhki	–	$1.12 \cdot 10^{-3}$
6	Guevara	–	$1.18 \cdot 10^{-3}$
7	Optimal FOPDT	–	$2.71 \cdot 10^{-3}$
	$N_S = 1,501$		

Table 6
Relative performance index values $S_{1,j}$ determined using different identification procedures ($j = 1, ..., 6$) compared to the proposed method ($j = 1$) for the process P_1.

j	Compared techniques	$S_{1,j}$	Improvement
1	Proposed-Proposed	1.0000	–
2	Proposed-Mittag-Leffler	0.9688	3%
3	Proposed-Symmetrical	0.5762	42%
4	Proposed-Asymmetrical	0.6847	31%
5	Proposed-Tavakoli-Kakhki	0.6570	34%
6	Proposed-Guevara	0.6279	37%
7	Proposed-Optimal FOPDT	0.2732	73%

at the cost of a larger execution time, which indicates a higher computational effort. The present black box model is two order of magnitude most faster than other robust meta-heuristic techniques. This outperformance of the current methodology could be explained by the fact that only one variable is optimized; meta-heuristics with a large number of variables are likely to do considerably better.

In conclusion, the results of this example demonstrate that the accuracy of the FFOPDT model estimated using the proposed hybrid approach is significantly better than that of the analytical methods. Additionally, the proposed approach provides a compromise between the accuracy of the identified model and the computational effort required. Indeed, the proposed hybrid method preserves the simplicity of the procedure when compared to other identification procedures.

4.2. Example 2

In this case, a higher-order lag-dominated fractional-order process model suggested in [13] is employed:

$$P_2(s) = \frac{K_2}{(1 + T_2 s^{\lambda_2})^n}, \tag{23}$$

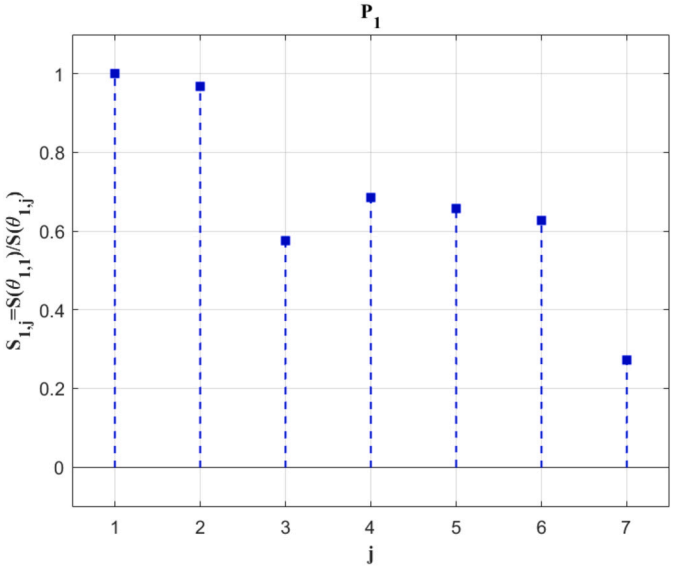

Fig. 11. Comparison based on the relative performance index between the results obtained using different identification procedures ($j = 1, ..., 6$) and the one obtained using the proposed procedure ($j = 1$) for the process P_1.

where $K_2 = 2$, $T_2 = 1$ s, $n = 5$, and $\lambda_2 = 0.85$.

Firstly, the proposed hybrid approach is used to estimate the FFOPDT model. An open-loop step-test experiment is applied to the process P_2 to obtain the reaction curve of the process, as illustrated in Fig. 12. Table 9 presents the process data required for the proposed identification procedure.

The FFOPDT model parameters for the proposed hybrid approach can be determined by utilizing process data in Table 9. Fig. 13 shows both the reaction curve of the process P_2 and the step response of the FFOPDT model estimated using the suggested identification technique.

In addition, several FFOPDT models for the process P_2 have also been obtained using various fractional identification methods. More specifically, FFOPDT models have been obtained using the methods based on the reaction curve of the process proposed by Gude et al. in [24], in [22] for the symmetrical set of representative points (10-50-90%), and in [23] for the asymmetrical set of points (10-65-90%), respectively. Finally, FFOPDT models have also been estimated following the three strategies followed by Tavakoli-Kakhki in [13].

Table 10 contains model parameters $\theta_{2,j} = \{K_{2,j}, T_{2,j}, L_{2,j}, \alpha_{2,j}, \}$ for $j = 1, ..., 7$, which have been obtained using the corresponding identification methods mentioned above.

The values of $S(\theta_{2,j})$ have been calculated for the models estimated using various identification procedures ($j = 1, ..., 7$) applied to the process P_2. These values provide an evaluation of the different identified models' accuracy, as illustrated in Fig. 14 and in Table 11. Additionally, Table 12 and Fig. 15 show the relative performance index values

Table 7
FFOPDT model parameters estimated for the process P_1 using various optimization-based identification techniques ($j = 1, ..., 5$).

j	Technique	FFOPDT model parameters $\theta_{1,j}$			
1	Proposed	$K_{1,1} = 3.0000$	$T_{1,1} = 5.6900$ s	$L_{1,1} = 1.5000$ s	$\alpha_{1,1} = 0.9155$
2	Optimization (ABC)	$K_{1,2} = 2.9605$	$T_{1,2} = 5.7192$ s	$L_{1,2} = 1.8766$ s	$\alpha_{1,2} = 0.9355$
3	Optimization (GWO)	$K_{1,3} = 2.9740$	$T_{1,3} = 5.5872$ s	$L_{1,3} = 1.6050$ s	$\alpha_{1,3} = 0.9163$
4	Optimization (PSO)	$K_{1,4} = 2.9711$	$T_{1,4} = 5.9463$ s	$L_{1,4} = 1.5194$ s	$\alpha_{1,4} = 0.9331$
5	Optimization (WOA)	$K_{1,5} = 2.9252$	$T_{1,5} = 6.5324$ s	$L_{1,5} = 1.9893$ s	$\alpha_{1,5} = 1.0039$

Table 8
Time-domain performance index values $S(\theta_{1,j})$ determined with the models estimated using different identification methods for the process P_1.

j	Technique	$S(\theta_{1,j})$	Execution time
1	Proposed	$7.39 \cdot 10^{-4}$	0.67 s
2	Optimization (ABC)	$5.78 \cdot 10^{-4}$	71.87 s
3	Optimization (GWO)	$4.13 \cdot 10^{-4}$	37.61 s
4	Optimization (PSO)	$3.64 \cdot 10^{-4}$	37.68 s
5	Optimization (WOA)	$2.20 \cdot 10^{-3}$	36.67 s
	$N_S = 1,501$		

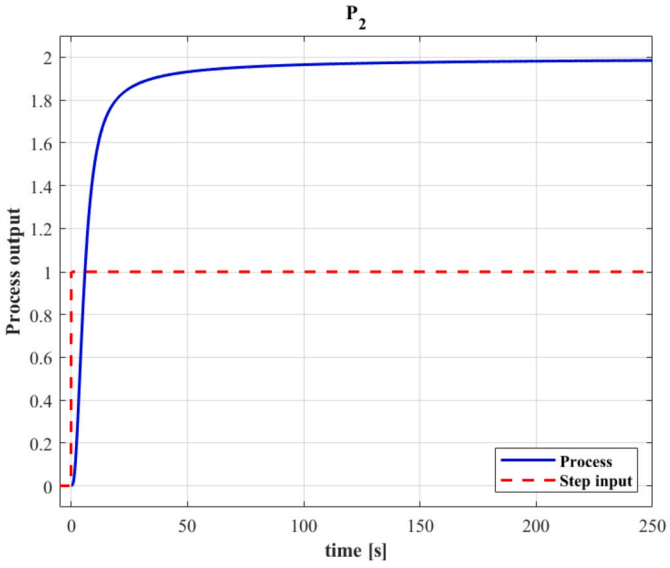

Fig. 12. Result of the open-loop step-test applied to process P_2: Step-input signal and process reaction curve.

Table 9
Process information obtained from the process reaction curve and required for FFOPDT model identification of process P_2.

Process $P_2(s)$
Proposed method ($x_1 = 10\%$, $x_3 = 90\%$)
$\Delta u = 1.00$
$\Delta y = 2.00$
$t_{10} = 2.3450$ s
$t_{90} = 19.200$ s

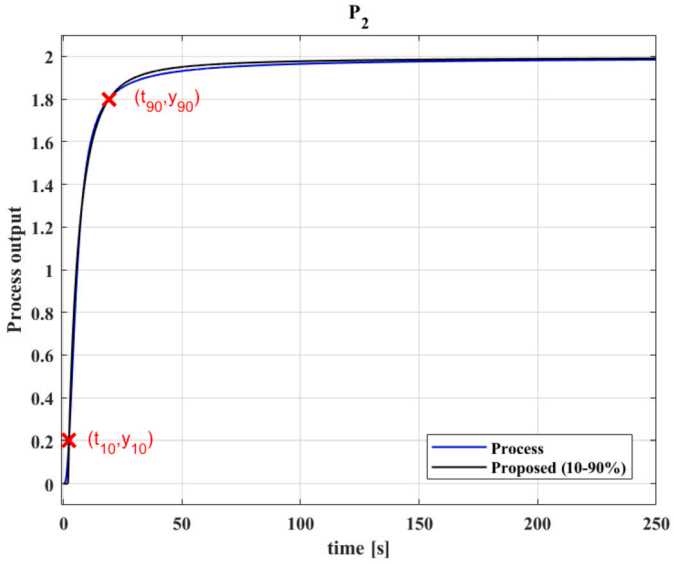

Fig. 13. Step response of the FFOPDT model estimated with the suggested identification procedure and reaction curve of the process for P_2. Points $x_1 = 10\%$ and $x_3 = 90\%$ are also included in the figure for illustrative purposes.

$S_{2,j} = S(\theta_{2,1})/S(\theta_{2,j})$ for the different models ($j = 1, ..., 7$) in comparison with that obtained with the proposed method ($j = 1$).

This figure illustrates that the proposed method reduces the value of S by 4%, 38%, 3%, 75%, 76%, and 90% compared to the procedures proposed by Gude with the Mittag-Leffler based method, for the symmetrical method, for the asymmetrical method, and by Tavakoli-Kakhki using three different strategies, respectively.

The parameters of several FFOPDT models for the process P_2 have also been estimated using the same optimization-based identification methods than for the previous example, i.e., ABC, GWO, PSO, WOA techniques have been used. Table 13 contains the parameters of the FFOPDT model $\theta_{2,j} = \{K_{2,j}, T_{2,j}, L_{2,j}, \alpha_{2,j}\}$ for $j = 1, ..., 5$.

In Table 14, the time-domain model performance index values $S(\theta_{2,j})$ and the execution time of the optimization-based procedures have been computed for the models estimated using various identification methods ($j = 1, ..., 5$) applied to process P_2.

4.3. Example 3

In this section, we use a thermal-based experimental prototype that has recently been constructed for teaching and research purposes [57].

The thermal process takes place in the upper part of the apparatus, which consists of a 3D-printer extruder head inside a methacrylate duct. The equipment also has a fan installed in front of the hot end.

Fig. 16 illustrates the appearance of the thermal experimental prototype, detailing the extruder head, its different parts, and the various forms of heat transfer that provides the controlled process its fractional behavior.

Table 10
FFOPDT model parameters for the process P_2 estimated using various identification techniques ($j = 1, ..., 7$).

j	Technique	FFOPDT model parameters $\theta_{2,j}$			
1	Proposed	$K_{2,1} = 2.00$	$T_{2,1} = 4.29$ s	$L_{2,1} = 2.01$ s	$\alpha_{2,1} = 0.877$
2	Gude Mittag-Leffler [24]	$K_{2,2} = 2.00$	$T_{2,2} = 4.44$ s	$L_{2,2} = 2.00$ s	$\alpha_{2,2} = 0.884$
3	Gude Symmetrical [22]	$K_{2,3} = 2.00$	$T_{2,3} = 5.07$ s	$L_{2,3} = 1.89$ s	$\alpha_{2,3} = 0.912$
4	Gude Asymmetrical [23]	$K_{2,4} = 2.00$	$T_{2,4} = 4.34$ s	$L_{2,4} = 2.00$ s	$\alpha_{2,4} = 0.879$
5	Tavakoli-Kakhki 1 [13]	$K_{2,5} = 2.00$	$T_{2,5} = 5.00$ s	$L_{2,5} = 1.50$ s	$\alpha_{2,5} = 0.850$
6	Tavakoli-Kakhki 2 [13]	$K_{2,6} = 2.00$	$T_{2,6} = 5.00$ s	$L_{2,6} = 0.69$ s	$\alpha_{2,6} = 0.850$
7	Tavakoli-Kakhki 3 [13]	$K_{2,7} = 2.00$	$T_{2,7} = 4.48$ s	$L_{2,7} = 1.50$ s	$\alpha_{2,7} = 0.850$

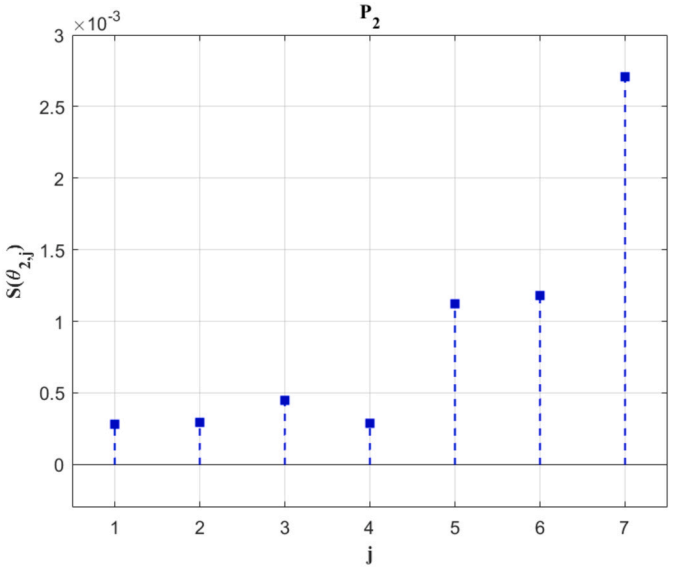

Fig. 14. Illustration of the performance index values $S(\theta_{2,j})$ determined with the models estimated using different identification methods for process P_2.

Table 11
Time-domain performance index values $S(\theta_{2,j})$ determined with the models estimated using different identification methods for the process P_2.

j	Technique	Set of points	$S(\theta_{2,j})$
1	Proposed	(10-90%)	$2.80 \cdot 10^{-4}$
2	Gude Mittag-Leffler	(10-90%)	$2.91 \cdot 10^{-4}$
3	Gude Symmetrical	(10-50-90%)	$4.49 \cdot 10^{-4}$
4	Gude Asymmetrical	(10-65-90%)	$2.90 \cdot 10^{-4}$
5	Tavakoli-Kakhki 1	–	$1.12 \cdot 10^{-3}$
6	Tavakoli-Kakhki 2	–	$1.18 \cdot 10^{-3}$
7	Tavakoli-Kakhki 3	–	$2.71 \cdot 10^{-3}$
	$N_S = 2,501$		

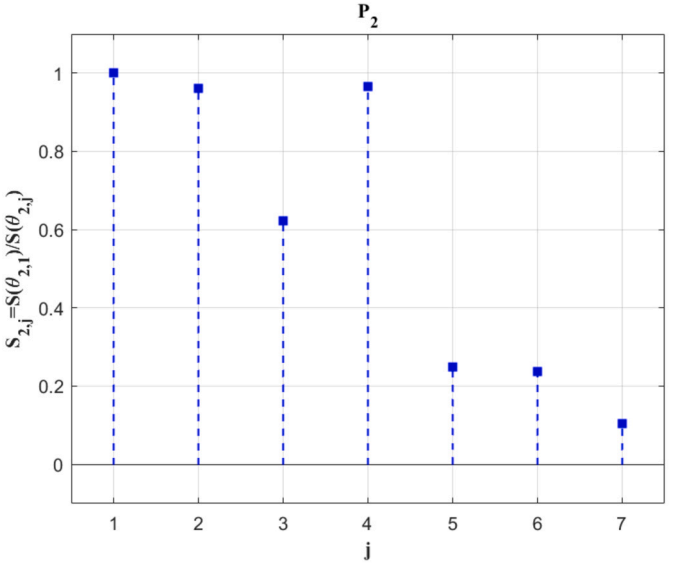

Fig. 15. Comparison based on the relative performance index between the results obtained using different identification procedures ($j = 1, ..., 7$) and the one obtained with the proposed procedure ($j = 1$) for the process P_2.

Table 12
Relative performance index values $S_{2,j}$ determined using different identification procedures ($j = 1, ..., 7$) compared to the proposed procedure ($j = 1$) for the process P_2.

j	Compared technique	$S_{1,j}$	Improvement
1	Proposed-Proposed	1.0000	–
2	Proposed-Mittag-Leffler	0.9622	4%
3	Proposed-Symmetrical	0.6236	38%
4	Proposed-Asymmetrical	0.9655	3%
5	Proposed-Tavakoli-Kakhki 1	0.2500	75%
6	Proposed-Tavakoli-Kakhki 2	0.2373	76%
7	Proposed-Tavakoli-Kakhki 3	0.1033	90%

One of the versatile features of this experimental prototype is that the control hardware can control both the heating power of the resistor inside the extruder head and the speed of the air fan. Therefore, the controlled process is configurable. The configuration considered in this work uses the air fan as the actuator while the heating resistor is kept constant.

The scheme in Fig. 17 illustrates the thermal-based experimental setup. It distinguishes the prototype, which below presents the block diagram of the controlled process, the hardware, where the proposed hybrid identification procedure is implemented, and the local PC, where the graphical user interface is shown. A microprocessor, which is part of the hardware architecture proposed in [57], is employed in this work as hardware for the implementation of the hybrid algorithm.

The reader is referred to [25] for a more detailed description of the benefits of this hardware architecture compared to other potential options.

The procedure followed consists of an open-loop step-test experiment. First, the control signal to the air fan is $u_F = 40\%$ and the command signal to the heating resistor is $u_H = 100\%$. A step change with amplitude $\Delta u_F = -20\%$ is applied at $t = 0$ s, while the command signal

Table 13
FFOPDT model parameters estimated for the process P_2 using various optimization-based identification techniques ($j = 1, ..., 5$).

j	Technique	Model parameters $\theta_{2,j}$			
1	Proposed	$K_{2,1} = 2.0000$	$T_{2,1} = 4.2873$ s	$L_{2,1} = 2.0100$ s	$\alpha_{2,1} = 0.8773$
2	Optimization (ABC)	$K_{2,2} = 1.9873$	$T_{2,2} = 4.8388$ s	$L_{2,2} = 1.7042$ s	$\alpha_{2,2} = 0.9110$
3	Optimization (GWO)	$K_{2,3} = 1.9843$	$T_{2,3} = 4.0981$ s	$L_{2,3} = 2.1914$ s	$\alpha_{2,3} = 0.8803$
4	Optimization (PSO)	$K_{2,4} = 1.9807$	$T_{2,4} = 4.4643$ s	$L_{2,4} = 2.0602$ s	$\alpha_{2,4} = 0.8974$
5	Optimization (WOA)	$K_{2,5} = 1.9554$	$T_{2,5} = 3.7290$ s	$L_{2,5} = 4.0917$ s	$\alpha_{2,5} = 0.9442$

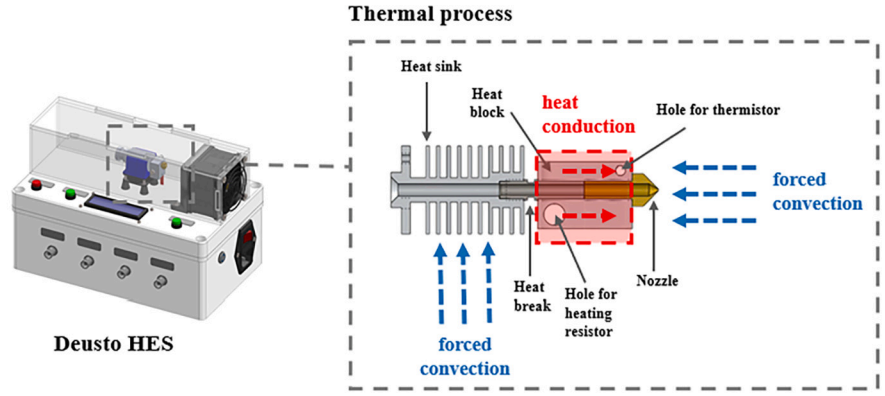

Fig. 16. Detail of the thermal process taking place in the extruder head and image of the experimental prototype.

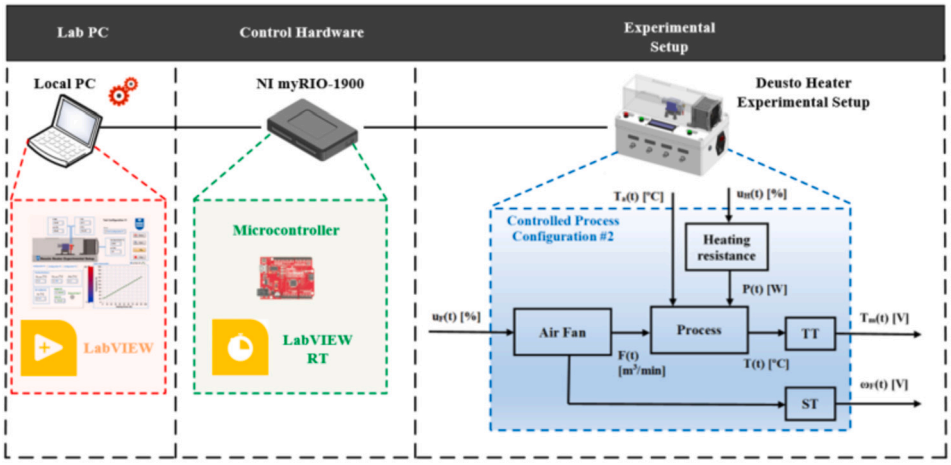

Fig. 17. Diagram of the thermal-based experimental setup, which includes the prototype and the microprocessor-based hardware. This figure also includes a local PC.

Table 14
Time-domain performance index values $S(\theta_{2,j})$ determined with the models estimated using different identification methods for the process P_2.

j	Technique	$S(\theta_{2,j})$	Execution time
1	Proposed hybrid approach	$2.80 \cdot 10^{-4}$	0.57 s
2	Optimization (ABC)	$3.69 \cdot 10^{-4}$	137.06 s
3	Optimization (GWO)	$2.59 \cdot 10^{-4}$	69.08 s
4	Optimization (PSO)	$2.27 \cdot 10^{-4}$	71.65 s
5	Optimization (WOA)	$5.50 \cdot 10^{-3}$	73.01 s
	$N_S = 2,501$		

Table 15
Process information collected from the process reaction curve and required for FFOPDT model identification of experimental controlled process.

Experimental Setup
Proposed method ($x_1 = 10\%$, $x_3 = 90\%$)
$\Delta u = \Delta u_F = -20\%$
$\Delta y = \Delta T_m = 26°C$
$t_{10} = 8.30$ s
$t_{90} = 130.50$ s

u_H is kept constant, as depicted in Fig. 18. The measured temperature at the thermal block $T_m(t)$, which is recorded in Fig. 19, is the process reaction curve and varies from 113.75 to 139.75°C ($\Delta T_m = 26°C$). Table 15 contains the information taken from the process reaction curve that is necessary to apply the proposed identification method.

Table 16
FFOPDT model parameters obtained for the experimental thermal-based controlled process using the proposed identification method and the ones obtained using the identification method proposed in [23] considering $x_1 = 10\%$ and $x_3 = 90\%$ and moving the location of x_2 ($x_2 = 50\%$ and $x_2 = 65\%$).

j	Technique	FFOPDT model parameters $\theta_{3,j}$			
1	Proposed	$K_{3,1} = 1.30°C/\%$	$T_{3,1} = 42.02$ s	$L_{3,1} = 3.50$ s	$\alpha_{3,1} = 0.957$
2	Gude Symmetrical [21]	$K_{3,2} = 1.30°C/\%$	$T_{3,2} = 39.52$ s	$L_{3,2} = 3.82$ s	$\alpha_{3,2} = 0.948$
3	Gude Asymmetrical [23]	$K_{3,3} = 1.30°C/\%$	$T_{3,3} = 39.93$ s	$L_{3,3} = 3.76$ s	$\alpha_{3,3} = 0.949$

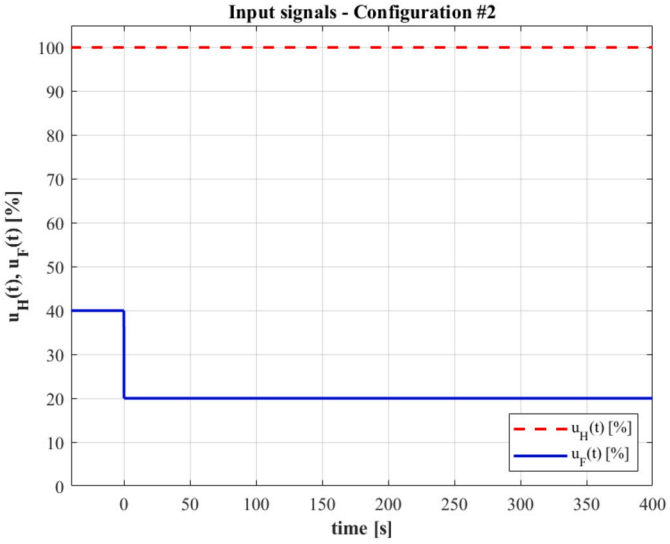

Fig. 18. Input signals applied in an open-loop step-test experiment: command signal to the heating resistor $u_H(t)[\%]$ and control signal to the air fan $u_F(t)[\%]$.

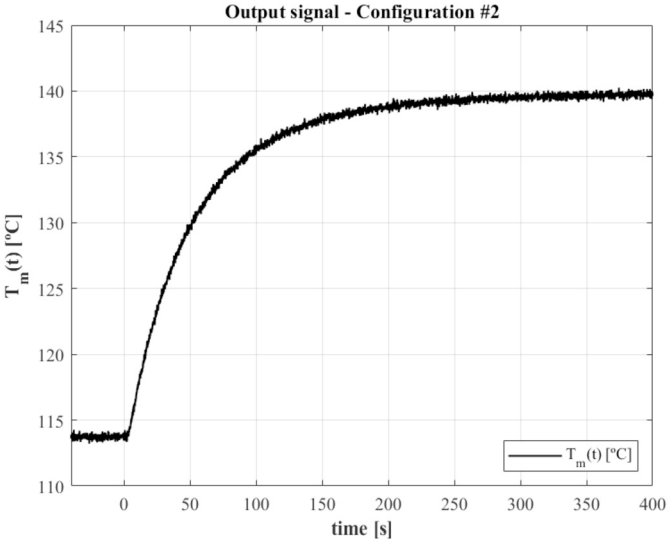

Fig. 19. Output signal obtained with an open-loop step-test experiment: process reaction curve $T_m(t)[°C]$.

Table 16 contains the FFOPDT model parameters estimated using the hybrid approach proposed in this paper and those obtained using the analytical methods developed by Gude and García Bringas in [21] and by Gude in [23] considering both the symmetrical (10-50-90%) and the asymmetrical (10-65-90%) set of representative points, respectively.

Fig. 20 compares the process reaction curve obtained using an open-loop step-test experiment with the step response of the FFOPDT model estimated with the suggested hybrid approach. The figure also illustrates the representative points ($x_1 = 10\%$ and $x_3 = 90\%$) on the reaction curve.

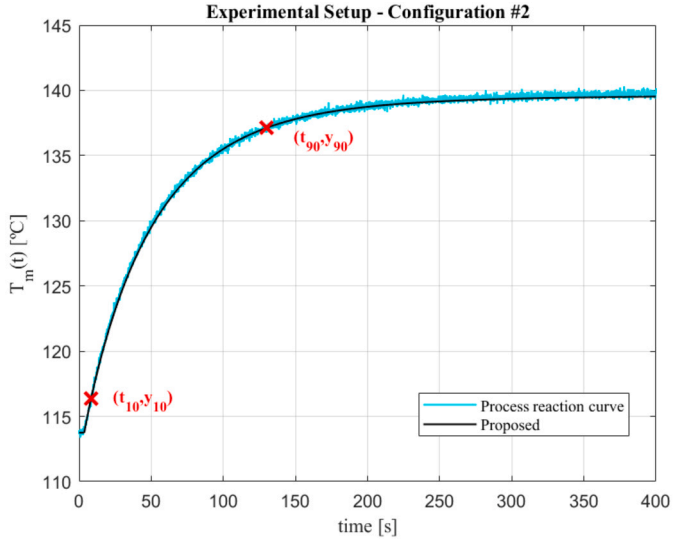

Fig. 20. Process reaction curve for P_1 and step response of the FFOPDT model estimated using the proposed identification procedure. Points $x_1 = 10\%$ and $x_3 = 90\%$ are also included in the figure for illustrative purposes.

Table 17
Time-domain performance index values $S(\theta_{3,j})$ obtained for the experimental thermal-based controlled process using different identification procedures.

j	Technique	Set of points	$S(\theta_{3,j})$
1	Proposed	(10-90%)	$4.8279 \cdot 10^{-5}$
2	Gude Symmetrical	(10-50-90%)	$6.1586 \cdot 10^{-3}$
3	Gude Asymmetrical	(10-65-90%)	$5.6591 \cdot 10^{-3}$
		$N_S = 4,001$	

The performance index values $S(\theta_{3,j})$ for the different identification procedures ($j = 1, 2, 3$) applied to the temperature-based controlled process are shown in Table 17.

The results obtained using the hybrid approach are significantly better in terms of accuracy than those obtained using the symmetrical and asymmetrical analytical procedures. The computational effort of the hybrid approach is higher than that of the analytical procedures, although searching only for the optimal value of the α parameter provides a significant improvement at the cost of moderate computational effort.

4.4. Discussion

Several examples have been used in this section to illustrate the applicability and effectiveness of the proposed hybrid approach. The first two illustrative examples serve to verify the good results obtained with the proposed identification procedure, in contrast to other methods

relying on the reaction curve of the process. Alternatively, the third example verifies the applicability of this procedure by implementing the proposed approach on a microprocessor-based hardware and applied to a temperature-based experimental prototype.

The hybrid approach proposed in this work has been compared with different identification procedures, some analytical and others based on optimization. The potential advantages of this procedure are discussed below.

- Examples 1 and 2 have demonstrated that the hybrid procedure provides more accurate FFOPDT models than those estimated using analytical methods based on the reaction curve of the process.
- Among these analytical methods, the method suggested by Gude and collaborators in [24] that estimates the parameter α using the asymptotic property of the Mittag-Leffler function is remarkable. Note that this approach provides an analytical technique to accurately determine the α-parameter. Since the way of estimating the parameters K, T, and L are the same as in the proposed procedure, the low value of the time-domain performance index S indicates that the estimated α value is very close to the optimum.
- Furthermore, obtaining very accurate FFOPDT models using the proposed approach, i.e. those with low values of S, confirms the hypothesis that parameter α is the most significant parameter for accurately fitting the step response of the identified fractional model to the process reaction curve.
- Additionally, the optimal FOPDT model has also been included in Example 1 to verify that the FFOPDT model significantly outperforms integer-order optimal models. This supports the known advantage derived from using reduced-order fractional models, which is documented in several technical references in terms of more accurate models; see, e.g., [12], [18], and [19].
- Examples 1 and 2 have also compared the FFOPDT model estimated using the proposed hybrid approach with several methods using various optimization techniques. In such examples, it is shown that this method provides good results, in some cases even outperforming some optimization-based methods. Note that the proposed hybrid method computes the optimal value of a single variable of the model, while optimization-based methods compute the optimal values of all the parameters of the FFOPDT model. The accuracy of the models estimated with more complex procedures is expected to improve at the cost of increasing the computational effort and the complexity of the procedure, as can be observed from the results obtained in the previous sections.
- In relation to optimization-based methods, it should be noted that they generally require good initial settings of the model parameters. Given that analytical methods based on three symmetrical or asymmetrical points on the process reaction curve generally provide good results in terms of accuracy with minimal computational effort, these model parameters can be used as initial values in an optimization-based identification procedure.
- Example 3 has been used to gain insight into the practical application of fractional identification algorithms on real-time targets [23]. For this purpose, the control hardware architecture proposed in [25] has been used to validate the applicability and effectiveness of the proposed hybrid algorithm applied to a temperature-based experimental setup. Furthermore, this example contributes to bridging the gap between real-time hardware solutions and software-based fractional modeling simulations [23].

Since fractional behavior is ubiquitous in industrial processes, see [58] and [26], the availability of methods for the identification of reduced-order fractional models and the capability to be deployed on real-time targets is a requirement of industry [59]. In the context of this work, an interesting discussion arises as to whether the extra effort of considering optimization to obtain a more accurate model is worth it. In this regard, it is important to note that the mathematical background of plant technicians and operators is generally limited and that a typical process plant usually includes a large number of control loops. Therefore, for such a new identification method to have a potential impact on industry, key requirements are simplicity and a trade-off between the accuracy of the identified fractional model and the computational effort required for its implementation on an industrial-level hardware device.

In conclusion, the industry requires simple-to-apply fractional-order model identification procedures that are easy-to-implement on a hardware device. The authors believe that these characteristics are fulfilled by the procedure proposed in this work while providing the required balance between accuracy and computational effort.

5. Conclusions

This work presents a new method for identifying reduced-order fractional models applied to describe the dynamic behavior of processes with overdamped step response.

The proposed approach uses information collected from the reaction curve of the process, which was obtained by applying an open-loop step-test experiment. The proposed method is hybrid because it combines single-variable optimization techniques and analytical expressions for the estimation of model parameters.

The results obtained with the examples in this paper prove the effectiveness of this hybrid approach in the identification of fractional models. It also demonstrates the applicability of the hybrid approach and the straightforwardness of its practical implementation on microprocessor-based hardware by being applied to a temperature-based experimental setup.

The authors believe that this hybrid approach that finds an appropriate balance between the simplicity of the procedure and the accuracy of the identified model will promote the adoption of this type of reduced-order fractional models at the industrial level.

In the context of the research presented in this paper, the following future work can be suggested:

- The proposed approach is restricted to fractional order values in the range $0.5 \leq \alpha \leq 1.0$, a natural extension to this work is to apply it to the range $1.0 \leq \alpha \leq 2.0$, i.e., for processes with underdamped behavior.
- Although microprocessor-based hardware has been used in this work for the implementation of the proposed fractional-order identification algorithm, it is well known that the Programmable Logic Controller (PLC) is the most widespread device in the process industry. A future work aims to implement this identification procedure in a PLC.

CRediT authorship contribution statement

Juan J. Gude: Writing – review & editing, Writing – original draft, Validation, Software, Methodology, Investigation, Data curation, Conceptualization. **Pablo García Bringas:** Supervision, Project administration, Methodology, Investigation, Funding acquisition, Conceptualization. **Marco Herrera:** Writing – review & editing, Writing – original draft, Validation, Software, Methodology, Investigation. **Luis Rincón:** Writing – review & editing, Validation, Methodology, Investigation. **Antonio Di Teodoro:** Writing – review & editing, Methodology, Investigation, Formal analysis. **Oscar Camacho:** Writing – review & editing, Supervision, Methodology, Investigation, Conceptualization.

Declaration of competing interest

The authors declare that they have no known competing financial interests or personal relationships that could have appeared to influence the work reported in this paper.

Data availability

No data was used for the research described in the article.

Acknowledgements

A. Di Teodoro and O. Camacho thank the Universidad San Francisco de Quito for supporting this work through the Poli-Grants Program under Grant 17965.

Juan J. Gude and Pablo García Bringas thank the Basque Government for its funding support through the BEREZ-IA Elkartek project (ref. KK-2023/00012).

References

[1] G.F. Franklin, J.D. Powell, A. Emami-Naeini, J.D. Powell, Feedback Control of Dynamic Systems, vol. 4, Prentice Hall, Upper Saddle River, 2002.
[2] C.A. Smith, A.B. Corripio, Principles and Practices of Automatic Process Control, John Wiley & Sons, 2005.
[3] L. Wang, From Plant Data to Process Control: Ideas for Process Identification and PID Design, vol. 11, CRC Press, 2000.
[4] K.J. Åström, T. Hägglund, Advanced PID control, in: ISA-The Instrumentation, Systems and Automation Society, 2006.
[5] A. Visioli, Practical PID Control, Springer Science & Business Media, 2006.
[6] A. O'dwyer, Handbook of PI and PID Controller Tuning Rules, World Scientific, 2009.
[7] O. Garpinger, T. Hägglund, K.J. Åström, Performance and robustness trade-offs in pid control, J. Process Control 24 (5) (2014) 568–577.
[8] U. Mehta, K. Bingi, S. Saxena, Applied Fractional Calculus in Identification and Control, Springer, 2022.
[9] J. Calaf-Chica, V. Cea-González, M.-J. García-Tárrago, F.-J. Gómez-Gil, Fractional viscoelastic models for the estimation of the frequency response of rubber bushings based on relaxation tests, Results Eng. 20 (2023) 101465.
[10] M.Ö. Efe, Fractional order systems in industrial automation—a survey, IEEE Trans. Ind. Inform. 7 (4) (2011) 582–591.
[11] C.I. Muresan, C.M. Ionescu, Generalization of the fopdt model for identification and control purposes, Processes 8 (6) (2020) 682.
[12] A. Tepljakov, Fractional-Order Modeling and Control of Dynamic Systems, Springer, 2017.
[13] M. Tavakoli-Kakhki, M. Haeri, M.S. Tavazoei, Simple fractional order model structures and their applications in control system design, Eur. J. Control 16 (6) (2010) 680–694.
[14] M. Tavakoli-Kakhki, M.S. Tavazoei, A. Mesbahi, Parameter and order estimation from noisy step response data, IFAC Proc. Vol. 46 (1) (2013) 492–497.
[15] M. Tavakoli-Kakhki, M. Saleh Tavazoei, Estimation of the order and parameters of a fractional order model from a noisy step response data, J. Dyn. Syst. Meas. Control 136 (3) (2014) 031020.
[16] H. Malek, Y. Luo, Y. Chen, Identification and tuning fractional order proportional integral controllers for time delayed systems with a fractional pole, Mechatronics 23 (7) (2013) 746–754.
[17] S. Ahmed, Parameter and delay estimation of fractional order models from step response, IFAC-PapersOnLine 48 (8) (2015) 942–947.
[18] B.B. Alagoz, A. Tepljakov, A. Ates, E. Petlenkov, C. Yeroglu, Time-domain identification of one noninteger order plus time delay models from step response measurements, Int. J. Model. Simul. Sci. Comput. 10 (01) (2019) 1941011.
[19] E. Guevara, H. Meneses, O. Arrieta, R. Vilanova, A. Visioli, F. Padula, Fractional order model identification: computational optimization, in: 2015 IEEE 20th Conference on Emerging Technologies & Factory Automation (ETFA), IEEE, 2015, pp. 1–4.
[20] H. Meneses, O. Arrieta, F. Padula, A. Visioli, R. Vilanova, Fopi/fopid tuning rule based on a fractional order model for the process, Fractal Fract. 6 (9) (2022) 478.
[21] J.J. Gude, P. García Bringas, Proposal of a general identification method for fractional-order processes based on the process reaction curve, Fractal Fract. 6 (9) (2022) 526.
[22] J.J. Gude, P. García Bringas, Influence of the selection of reaction curve's representative points on the accuracy of the identified fractional-order model, J. Math. (2022).
[23] J.J. Gude, Contributions to fractional-order modelling and control of dynamic systems: a theoretical and practical approach, Ph.D. thesis, 2023.
[24] J.J. Gude, A. Di Teodoro, O. Camacho, P. García Bringas, A new fractional reduced-order model-inspired system identification method for dynamical systems, IEEE Access 11 (2023) 103214–103231.
[25] J.J. Gude, P. García Bringas, A novel control hardware architecture for implementation of fractional-order identification and control algorithms applied to a temperature prototype, Mathematics 11 (1) (2022) 143.
[26] J. Sabatier, C. Farges, V. Tartaglione, Fractional Behaviours Modelling: Analysis and Application of Several Unusual Tools, vol. 101, Springer Nature, 2022.
[27] I. Podlubny, Fractional Differential Equations, Mathematics in Science and Engineering, Academic Press, New York, 1999.
[28] S. Das, Functional Fractional Calculus, vol. 1, Springer, 2011.
[29] A.A. Kilbas, H.M. Srivastava, J.J. Trujillo, Theory and Applications of Fractional Differential Equations, vol. 204, Elsevier, 2006.
[30] K.S. Miller, B. Ross, An Introduction to the Fractional Calculus and Fractional Differential Equations, Wiley, 1993.
[31] A.A. Kilbas, O. Marichev, S.G. Samko, Fractional Integrals and Derivatives (Theory and Applications), Gordon and Breach, Switzerland, 1993.
[32] I. Podlubny, Fractional-order systems and fractional-order controllers, Inst. Exp. Phys. Slovak Acad. Sci., Kosice 12 (3) (1994) 1–18.
[33] N. Coloma, A. Di Teodoro, D. Ochoa-Tocachi, F. Ponce, Fractional elementary bicomplex functions in the Riemann–Liouville sense, Adv. Appl. Clifford Algebras 31 (61) (2016).
[34] R. Gorenflo, A.A. Kilbas, F. Mainardi, S.V. Rogosin, et al., Mittag-Leffler Functions, Related Topics and Applications, Springer, 2020.
[35] S. Rogosin, The role of the Mittag-Leffler function in fractional modeling, Mathematics 3 (2) (2015) 368–381.
[36] J. Ceballos, N. Coloma, A. Di Teodoro, D. Ochoa-Tocachi, F. Ponce, Fractional multicomplex polynomials, Complex Anal. Oper. Theory 16 (4) (2022) 1–30.
[37] C. Audet, A Survey on Direct Search Methods for Blackbox Optimization and Their Applications, Springer, 2014.
[38] M.A. Muñoz, Y. Sun, M. Kirley, S.K. Halgamuge, Algorithm selection for black-box continuous optimization problems: a survey on methods and challenges, Inf. Sci. 317 (2015) 224–245.
[39] S. Ruder, An overview of gradient descent optimization algorithms, arXiv preprint arXiv:1609.04747.
[40] A. Chaturvedi, Handbook of Regression Analysis with Applications in R, Oxford University Press, 2022.
[41] D.S. Young, Handbook of Regression Methods, CRC Press, 2018.
[42] C. D'Ambrosio, A. Lodi, Mixed integer nonlinear programming tools: an updated practical overview, Ann. Oper. Res. 204 (2013) 301–320.
[43] N. Siddique, H. Adeli, Simulated annealing, its variants and engineering applications, Int. J. Artif. Intell. Tools 25 (06) (2016) 1630001.
[44] K. Amine, et al., Multiobjective simulated annealing: principles and algorithm variants, Adv. Oper. Res. (2019).
[45] T. Bartz-Beielstein, J. Branke, J. Mehnen, O. Mersmann, Evolutionary algorithms, Wiley Interdiscip. Rev. Data Min. Knowl. Discov. 4 (3) (2014) 178–195.
[46] A. Lambora, K. Gupta, K. Chopra, Genetic algorithm-a literature review, in: 2019 International Conference on Machine Learning, Big Data, Cloud and Parallel Computing (COMITCon), IEEE, 2019, pp. 380–384.
[47] T. Ting, X.-S. Yang, S. Cheng, K. Huang, Hybrid metaheuristic algorithms: past, present, and future, in: Recent Advances in Swarm Intelligence and Evolutionary Computation, 2015, pp. 71–83.
[48] J.C. Bansal, Particle swarm optimization, in: Evolutionary and Swarm Intelligence Algorithms, 2019, pp. 11–23.
[49] S. Greenhill, S. Rana, S. Gupta, P. Vellanki, S. Venkatesh, Bayesian optimization for adaptive experimental design: a review, IEEE Access 8 (2020) 13937–13948.
[50] R.H. Myers, D.C. Montgomery, G.G. Vining, C.M. Borror, S.M. Kowalski, Response surface methodology: a retrospective and literature survey, J. Qual. Technol. 36 (1) (2004) 53–77.
[51] N. Coloma, A. Di Teodoro, D. Ochoa-Tocachi, et al., Fractional elementary bicomplex functions in the Riemann–Liouville sense, Adv. Appl. Clifford Algebras 31 (2021) 63.
[52] A. Isaksson, S. Graebe, Derivative filter is an integral part of pid design, IEE Proc., Control Theory Appl. 149 (1) (2002) 41–45.
[53] V.R. Segovia, T. Hägglund, K.J. Åström, Measurement noise filtering for pid controllers, J. Process Control 24 (4) (2014) 299–313.
[54] J.J. Gude, E. Kahoraho, Modified Ziegler-Nichols method for fractional pi controllers, in: 2010 IEEE 15th Conference on Emerging Technologies & Factory Automation (ETFA 2010), IEEE, 2010, pp. 1–5.
[55] B. Lennartson, B. Kristiansson, Evaluation and tuning of robust pid controllers, IET Control Theory Appl. 3 (3) (2009) 294–302.
[56] D. Xue, Fractional-Order Control Systems: Fundamentals and Numerical Implementations, vol. 1, Walter de Gruyter GmbH & Co KG, 2017.
[57] J.J. Gude, P. García Bringas, Proposal of a control hardware architecture for implementation of fractional-order controllers, in: Proceedings of the 16th International Conference Dynamical Systems Theory and Applications (DSTA 2021), Lodz, Poland, 2021, pp. 6–9.
[58] Y. Chen, Ubiquitous fractional order controls?, IFAC Proc. Vol. 39 (11) (2006) 481–492.
[59] R. Caponetto, Fractional Order Systems: Modeling and Control Applications, vol. 72, World Scientific, 2010.